

A STATISTICAL MODEL OF ATMOSPHERIC
TEMPERATURE SIGNALS

Edward Marvin Kline

NAVAL POSTGRADUATE SCHOOL

Monterey, California



THESIS

A STATISTICAL MODEL OF
ATMOSPHERIC TEMPERATURE SIGNALS

by

Edward Marvin Kline

March 1972

Approved for public release; distribution unlimited.

A Statistical Model of
Atmospheric Temperature Signals

by

Edward Marvin Kline
Lieutenant, United States Navy
B.S., University of Idaho, 1967

Submitted in partial fulfillment of the
requirements for the degree of

MASTER OF SCIENCE IN OCEANOGRAPHY

from the

NAVAL POSTGRADUATE SCHOOL

ABSTRACT

The "ramp" is an often observed feature in temperature fluctuations during unstable atmospheric conditions. It is characterized by a gradual increase in temperature followed by a sudden drop to an ambient level. This ramp clearly distinguishes temperature signals from other turbulence signals such as velocity. Three different ramp-type atmospheric temperature fluctuations and their derivatives are constructed and statistically examined for the parameters skewness and coefficient of excess. These statistical values are compared with values obtained from actual signals. The "complex ramp signal" was found to represent these quite well. Skewness and coefficient of excess for this signal could be altered almost independently of each other. The complex ramp is constructed by inscribing nearly symmetrical consecutive triangles within two envelope rays of constant but different slopes such that the two envelope rays approximate a ramp function.

TABLE OF CONTENTS

I.	INTRODUCTION	8
	A. OBJECTIVE	8
	B. GENERAL FEATURES OF TEMPERATURE SIGNALS	9
II.	SIGNALS	13
	A. ATMOSPHERIC TEMPERATURE FLUCTUATIONS	13
	B. MODELS OF ATMOSPHERIC TEMPERATURE FLUCTUATIONS	13
III.	METHOD OF EXAMINATION	16
	A. SIGNAL	16
	B. DIFFERENTIATED SIGNALS	18
	C. STATISTICS APPLIED	19
IV.	RESULTS	26
V.	CONCLUSIONS	49
VI.	RECOMMENDATIONS FOR FURTHER STUDY	50
	COMPUTER PROGRAM	53
	BIBLIOGRAPHY	59
	INITIAL DISTRIBUTION LIST	61
	FORM DD 1473	62

LIST OF FIGURES

FIGURE 1:	Atmospheric Temperature and Differentiated Temperature Signal.	11
FIGURE 2:	Schematic of Convective Plume According to Gill (1971)	12
FIGURE 3:	Growth of Ramps as Atmosphere Changes from Stable to Unstable	15
FIGURE 4:	Standard Ramp Model and Differentiated Standard Ramp Model	22
FIGURE 5:	Asymmetrical Ramp Model and Differentiated Asymmetrical Ramp Model	23
FIGURE 6:	Complex Ramp Model and Differentiated Complex Ramp Model	24
FIGURE 7:	Variation of Standard Ramp Signal with Period	28
FIGURE 8:	Variation of Standard Ramp Signal with Ramp Width	31
FIGURE 9:	Variation of Standard Ramp Signal with Ramp Slope	31
FIGURE 10:	Variation of Asymmetrical Ramp Signal with Period	33
FIGURE 11:	Variation of Asymmetrical Ramp Signal with Ramp Width	34
FIGURE 12:	Variation of Asymmetrical Ramp Signal with Back Slope	34
FIGURE 13:	Variation of Asymmetrical Ramp Signal with Back Slope Width	38
FIGURE 14:	Variation of Complex Ramp Signal with Period	40
FIGURE 15:	Variation of Complex Ramp Signal with Upper Basic Slope	42

FIGURE 16:	Variation of Complex Ramp Signal with Lower Basic Slope	44
FIGURE 17:	Variation of Complex Ramp Signal with Ramp Width	46

LIST OF TABLES

TABLE I.	- SKEWNESS AND COEFFICIENT OF EXCESS OF DIFFERENTIATED TEMPERATURE SIGNALS	25
TABLE II.	- VARIATION OF DIFFERENTIATED RAMP SIGNAL WITH PERIOD	27
TABLE III.	- VARIATION OF DIFFERENTIATED RAMP SIGNAL WITH RAMP SLOPE	29
TABLE IV.	- VARIATION OF DIFFERENTIATED RAMP SIGNAL WITH RAMP WIDTH	30
TABLE V.	- VARIATION OF DIFFERENTIATED ASYMMETRICAL RAMP SIGNAL WITH PERIOD.	32
TABLE VI.	- VARIATION OF DIFFERENTIATED ASYMMETRICAL RAMP SIGNAL WITH BACK SLOPE	34
TABLE VII.	- VARIATION OF DIFFERENTIATED ASYMMETRICAL RAMP SIGNAL WITH RAMP WIDTH	35
TABLE VIII.	- VARIATION OF DIFFERENTIATED ASYMMETRICAL RAMP SIGNAL WITH BACK SLOPE WIDTH	37
TABLE IX.	- VARIATION OF DIFFERENTIATED COMPLEX RAMP SIGNAL WITH PERIOD	39
TABLE X.	- VARIATION OF DIFFERENTIATED COMPLEX RAMP SIGNAL WITH UPPER BASIC SLOPE	41
TABLE XI.	- VARIATION OF DIFFERENTIATED COMPLEX RAMP SIGNAL WITH LOWER BASIC SLOPE	43
TABLE XII.	- VARIATION OF DIFFERENTIATED COMPLEX RAMP SIGNAL WITH RAMP WIDTH	45
TABLE XIII.	- VARIATION OF DIFFERENTIATED COMPLEX RAMP SIGNAL WITH PERIOD AND RAMP WIDTH	47
TABLE XIV.	- VARIATION OF A DIFFERENTIATED VELOCITY SIGNAL WITH RAMP WIDTH	52

ACKNOWLEDGEMENT

The author would like to thank Professor N. E. J. Boston, whose appreciated advice and encouragement greatly contributed to this thesis. The author is also grateful to Professor K. L. Davidson for his willing assistance. Miss S. D. Raney of the W. R. Church Computer Center provided much needed programming advice and Professor A. L. Schoenstadt provided mathematical assistance. Finally, the author would like to thank his wife, Linda, who served as part-time typist and proof reader.

I. INTRODUCTION

A. OBJECTIVE

Atmospheric and oceanic turbulence contributes greatly to interactions at the air/sea interface. Mathematical models have been developed which attempt to describe this turbulent boundary layer where atmosphere and ocean meet. As sensing systems become more sophisticated and more turbulence data becomes available, existing models are accordingly modified. An important modification was made by Kolmogorov (1962) and others to account for rather large fluctuations observed in the energy dissipation rate. Such fluctuations were observed primarily in differentiated turbulence signals which emphasized high frequency components. Kolmogorov revised his theory in order to incorporate how the velocity derivative's skewness (s) and coefficient of excess (c.e.) increased with the Reynold's number (Re). In the energy containing region the parameters s and c.e. are zero since the turbulence fluctuations seem to have a Gaussian distribution. At small scales (high frequencies) they are decidedly not zero. The skewness and coefficient of excess of the derivative of the temperature fluctuations are not zero either. One might then ask, "Knowing s and c.e. from real data, is it possible to construct signals that resemble observed temperature signals?" Such was the objective of this thesis.

B. GENERAL FEATURES OF TEMPERATURE SIGNALS

The "ramp" is an often observed feature in temperature fluctuations during unstable atmospheric conditions. It is characterized by a gradual increase in temperature followed by a sudden drop to an ambient level. The signal rarely falls below this ambient level (Figure 1). This sudden drop clearly distinguishes a temperature signal from other turbulence signals such as velocity signals whose main perturbations from the ambient level are usually gradual rises with accompanying gradual descents. It seems natural to conclude that these observable non-Gaussian type features in temperature signals probably contribute to the measureable skewness and coefficient of excess.

Electronic pattern recognition studies of atmospheric temperature fluctuations have been made by Sokol (1971). Although his study was not exhaustive, he achieved over 70% detection success. Another method of describing these signals is statistically through skewness and coefficient of excess. Since these statistics are zero for Gaussian noise, their values would represent only the non-Gaussian character of the signal. Thus, it may be possible in the future to use the frequency and structure of the ramps as a measure of some meteorological conditions.

Kaimal and Businger (1970) and Gill (1971) have demonstrated, over land at least, that the ramps are manifestations of convective plumes present near the air/earth interface. A schematic of the plume and its relation to the ramp, by

Gill (1971), are shown in Figure 2. Taylor (1958) and Gill (1971) have shown that these ramps can be correlated to other ramps appearing simultaneously at different heights but with a slight offset owing to a tilt in the plume; presumably due to wind shear. Boston (1971) indicated that the ramps in the temperature signal often correlate with perturbations in velocity signals. Safley (1972) has related them to water waves and velocity signals.

Plumes form a significant feature in the atmospheric boundary layer. Although they are present only a small fraction of the time they may account for the majority of heat, moisture, and momentum exchange. Safley (1972) found that the plumes accounted for 10% of the signal but 32% of the heat flux. Furthermore, they cause random fluctuations in electromagnetic waves over line-of-sight paths. Of recent interest is the effect they have on laser beams. When beamed over water they exhibit a random walking at the target. This is of considerable importance if a laser beam is to be used in a variety of practical applications, such as fire control systems.

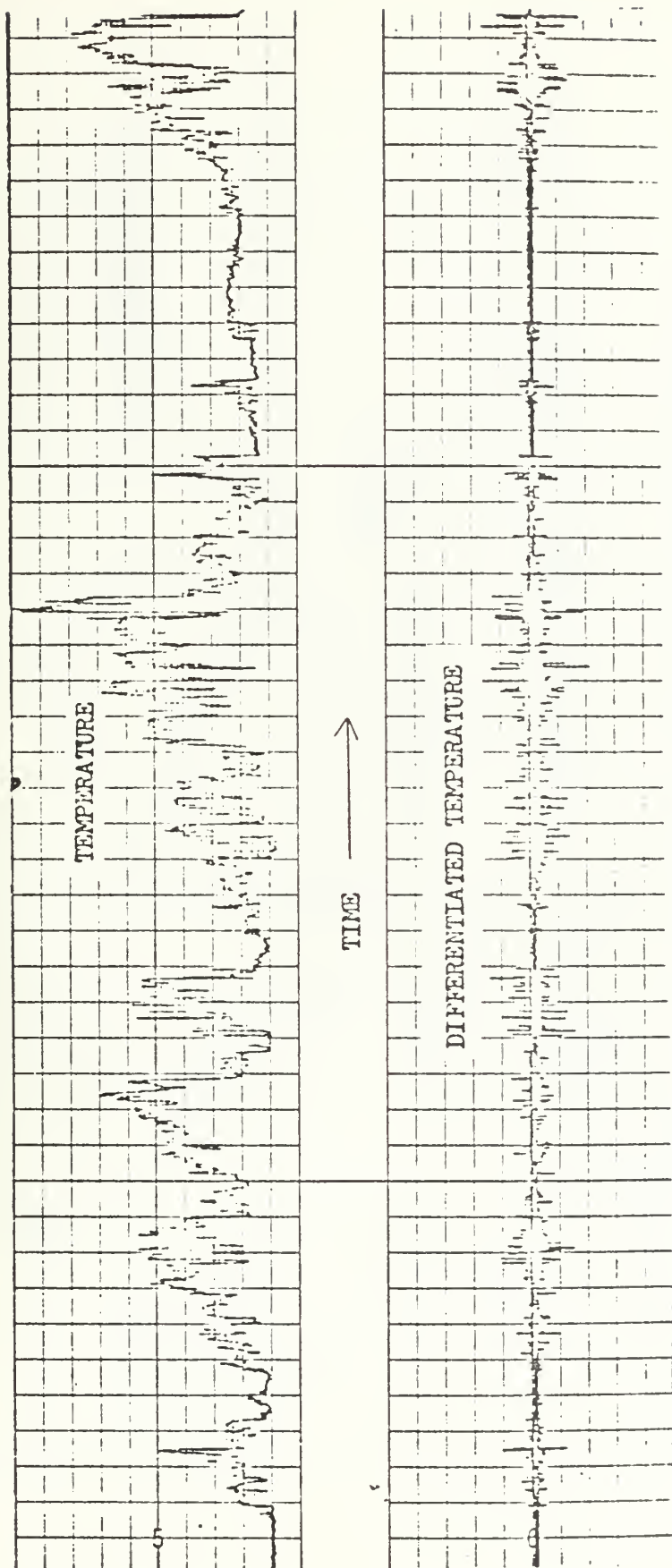


Fig. 1. Atmospheric Temperature and Differentiated Temperature Signal.

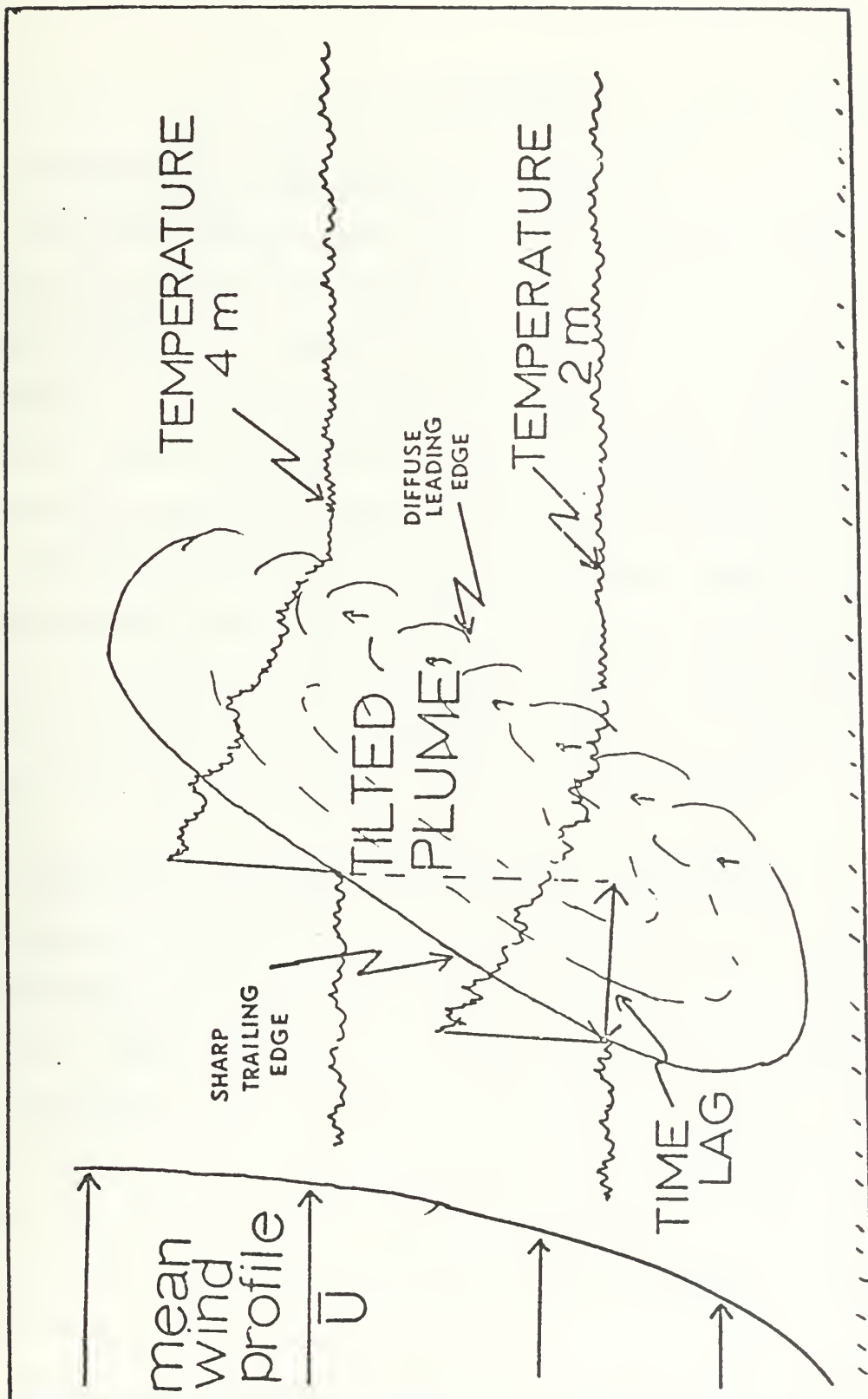


Fig. 2. Schematic of Convective Plume According to Gill (1971).

II. SIGNALS

A. ATMOSPHERIC TEMPERATURE FLUCTUATIONS

When the atmosphere is stable the temperature fluctuations tend to be small because the vertical turbulent velocity component tends to be damped out by the vertical temperature gradient. When the atmosphere is neutral the fluctuations are also small but tend to have both positive and negative excursions due to the lack of restoring buoyant forces.

Unstable conditions, on the other hand, exhibit the characteristic ramp features in the temperature trace (Figure 3). This is the condition that usually exists during the daytime in the lower atmosphere because the earth is heated and warms from below causing upward sensible heat transfer.

B. MODELS OF ATMOSPHERIC TEMPERATURE FLUCTUATIONS

Atmospheric turbulence for stable and neutral conditions is difficult to model since it is a broad band stochastic process. However, because of the characteristic ramp shape of temperature fluctuations in unstable conditions, some attractive possibilities for models present themselves. The model for the temperature signal of unstable conditions will consist of a basically straight line ramp signal to which variations will be added.

Rather than examining spectra of the modeled atmospheric temperature fluctuations, statistics of the derivative of the model will be examined. The differentiated signal emphasizes

the high frequency (high wave number) region of the signal which is the region of most interest in the modeling process since measurements in the last decade clearly indicate that the high wave number region is decidedly non-Gaussian. Also, visual inspection of ramps indicates that high frequency fluctuations may be important in ramp structures.

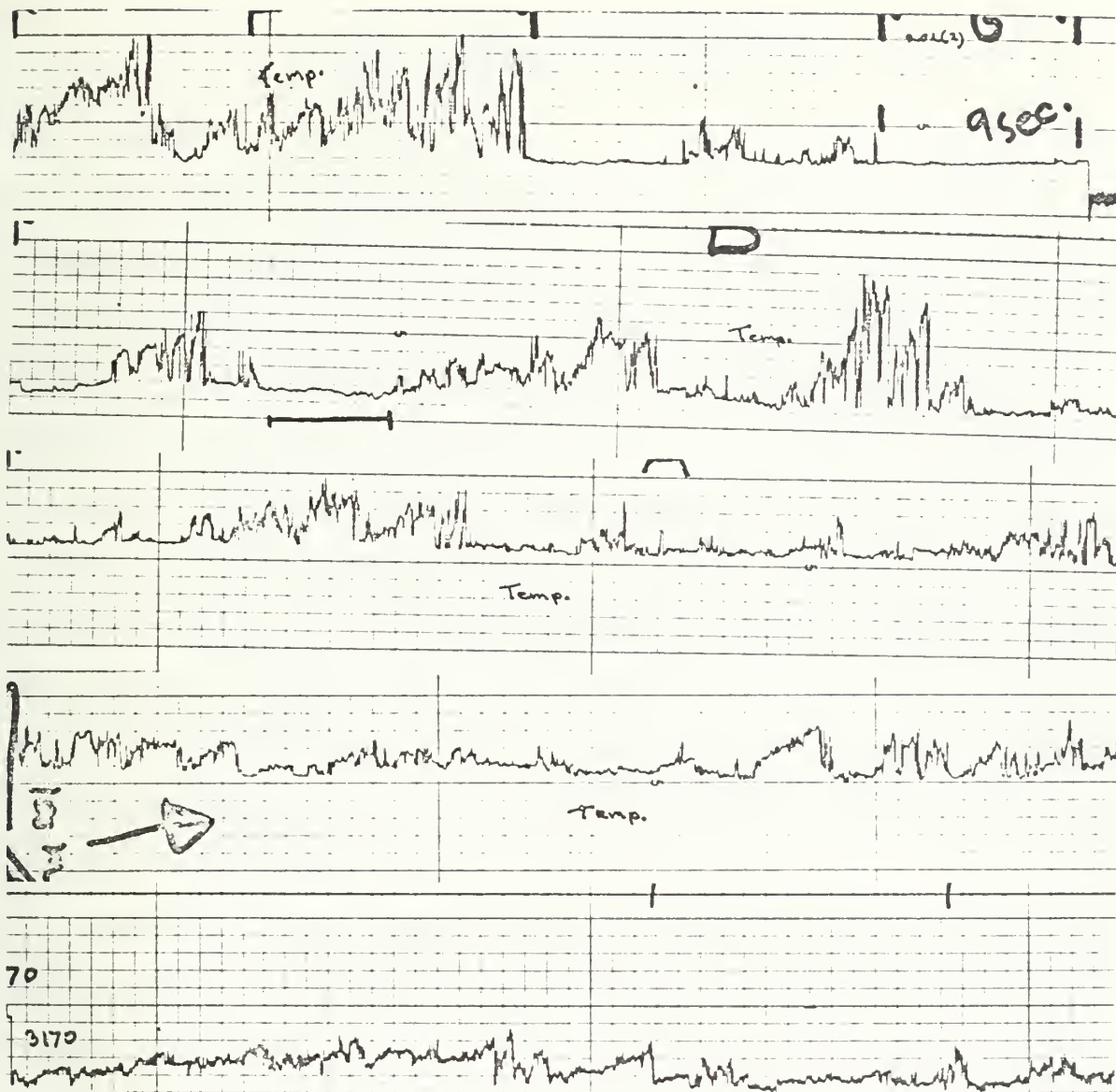


FIGURE 3. Growth of Ramps as Atmosphere Changes from Stable to Unstable (Bottom to Top).

III. METHOD OF EXAMINATION

A. SIGNAL

The signal modeling was done on an IBM 360/67 digital computer at the W. R. Church Computer Center, Naval Postgraduate School, Monterey, California. The basic ingredient in each model is the individual ramp which will be repeated at a specified interval. This collection of repetitive ramps will comprise the model signal. Each signal will be stored in a 10,000 X 1 vector array which represents the time axis of the signal. The size of the array may be varied, however, since the models are periodic. The distance between each array entry is constant and equal to the distance between samples of a digital recorder or converter (which is a function of the original sampling rate).

The models are dimensionless although voltage is implied and terms such as period and width must be redefined as they refer to digital words. Width refers to consecutive digital words or array entries and is used to describe the length of a ramp or a ramp component. Ramp period is the number of consecutive digital words between the start of a ramp and the start of the next succeeding ramp.

Three ramp modifications of increasing complexity will be examined as possible models for the temperature signal. The first is a "standard ramp signal" whose ramps are constructed of a gradual rise ending in a vertical drop (Figure 4) as

described by Gibson et al (1971). The variable parameters of this signal are (1) the period of the ramp, (2) the slope of the ramp, and (3) the width of the ramp.

The second modification is an "asymmetrical ramp" with a gradual rising front slope followed by a short steep back slope (Figure 5). The variables in this signal are (1) ramp period, (2) the back slope of the ramp, (3) ramp width, and (4) the width of the back slope. The front slope value and amplitude need not be included since they are functions of the other variables. Specifically,

$$\begin{aligned} \text{front slope} &= ((\text{back slope width}) \times (\text{back slope})) / \\ &((\text{ramp width}) - (\text{back slope width})), \text{ amplitude} = \\ &(\text{back slope}) (\text{back slope width}). \end{aligned}$$

The third modification, a "complex ramp", is constructed by inscribing nearly symmetrical consecutive triangles (teepees) within two envelope rays of constant but different slopes such that the two rays approximate a ramp function (Figure 6). Each succeeding slope of the inscribed teepees will be greater in absolute value and alternate in sign. This type of model is chosen because close inspection of temperature strip charts shows that large fluctuations of increasing amplitude is a commonly observed ramp feature. The variables for this signal are (1) ramp period, (2) slope of the upper defining ray, (3) slope of the lower defining ray, and (4) the width of the ramp. The period of the internal teepees is not listed as a variable because, as will be explained later, the model

is dimensionless and, for example, halving the period or doubling the frequency of the internal teepees can be accomplished by simultaneously doubling the ramp period and ramp width.

B. DIFFERENTIATED SIGNAL

As previously mentioned the differentiated signal will be examined since it emphasizes the higher frequencies that contribute to the non-Gaussian nature of the signals. Therefore, now that the direct signal has been modeled the differentiated signal must be computed. The differentiated standard ramp signal is merely a box function whose amplitude is equal to the slope of the ramp (Figure 4).

The differentiated asymmetrical ramp signal is an alternating asymmetrical box function. Each differentiated pulse consists of a broad positive box whose amplitude is equal to the front slope of the ramp followed by a short, highly negative box whose amplitude is equal to the back slope of the ramp (Figure 5).

The signal model for the derivative of the complex ramp (Figure 6) is constructed by letting

$\frac{dy}{dx} = \text{uslope (1)},$ the slope of the uppermost limiting ray and,

$\frac{dy'}{dx'} = \text{lslope (2)},$ the slope of the lowermost limiting ray.

For representation on a digital computer the implied distance between successive array entries is a mesh length. Then within the ramps each succeeding array entry represents successive slopes of the inscribed teepees. However, for purposes of computing these slopes the mesh length is offset by half its

length and the difference between successive intersections of the upper slope and the lower slope is computed. From equations (1) and (2),

$$dy = (dx)(uslope)$$

$$dy' = (dx')(lslope).$$

Let $n = dx_n$, where n is the number of mesh lengths along the time axis of the signal measured from the start of the ramp.

Hence,

$$dy_n = n(uslope)$$

$$dy'_n = n(lslope).$$

Therefore, assuming the first slope is positive:

$$x(n) = (n+1) (uslope) - (n) (lslope)$$

$$x(n+1) = (n+2) (lslope) - (n+1) (uslope)$$

$$x(n+2) = (n+3) (uslope) - (n+2) (lslope)$$

$$x(n+3) = (n+4) (lslope) - (n+3) (uslope)$$

$$x(n+4) = (n+5) (uslope) - (n+4) (uslope)$$

.

.

.

Note that the first and last values may have to be computed separately since the signal must be continuous with the ambient level at the beginning and end of the ramp. A sample program with this representation is given in a separate section.

C. STATISTICS APPLIED

One can usually discern a temperature signal from a velocity signal by the ramp. However, if the spectra of these signals are examined in the range of about 1 Hz to 1000 Hz they are

remarkably similar, although their statistics such as skewness and coefficient of excess are quite different. As a result, recent turbulence literature has used these two parameters extensively to describe turbulence signals. Therefore, skewness and coefficient of excess will be used as modeling parameters. The skewness and c.e. of the models will be compared to those of actual signals.

Skewness is a measure of the amount a signal differs from its mean value. The skewness of a Gaussian signal is zero. A distribution that is skewed to the right has a positive skewness and a distribution that is skewed to the left has a negative skewness. A symmetrical signal will have zero skewness and a signal with a high skewness value will have pulses that are very asymmetrical. Coefficient of excess is a measure of the peakedness of a distribution. A distribution that is less peaked than normal distribution has c.e. values less than zero, and vice versa. The c.e. of a signal is highly sensitive to infrequent deviations from the mean signal value. Therefore, a signal with ramps spaced relatively far apart will have a higher c.e. value than a signal with ramps spaced close together. These higher order statistics emphasize the higher frequencies which are non-Gaussian. However, since they are exponential functions, they require a longer record to achieve stable results. Therefore, the use of statistics of orders higher than c.e. is somewhat limited.

Skewness (s) is defined as :

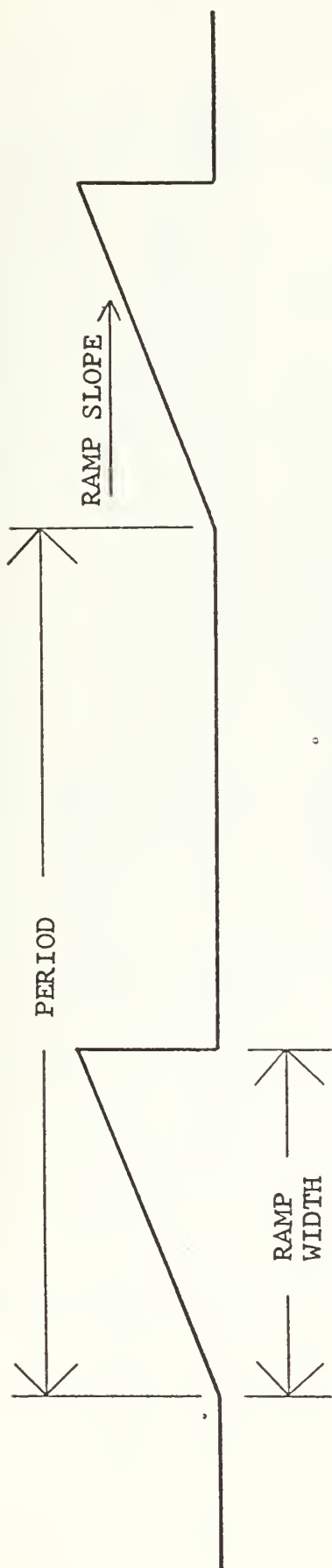
$$s = e^3 / (e^2)^{3/2},$$
 where e is the variation of the signal from its mean value.

Coefficient of excess (c.e.) is defined as:

$$\text{c.e.} = \frac{e^4}{(e^2)^2} - 3. \text{ Often one sees } e^4/(e^2)^2, \text{ the ratio}$$

of the fourth moment to the second moment, used as a statistic and referred to as "kurtosis," but c.e. will be used here because it is zero for a Gaussian signal.

The skewness and c.e. for differentiated temperature signals have been computed by several people (Table I). Although the one thing the statistics seem to have in common is their variability, representative figures can be chosen. For temperature signal a skewness value between 0.2 and 0.5 seems common and likewise a value for c.e. is about 30. Compare these values to representative velocity signal values of -0.5 and 15 for s and c.e. respectively.

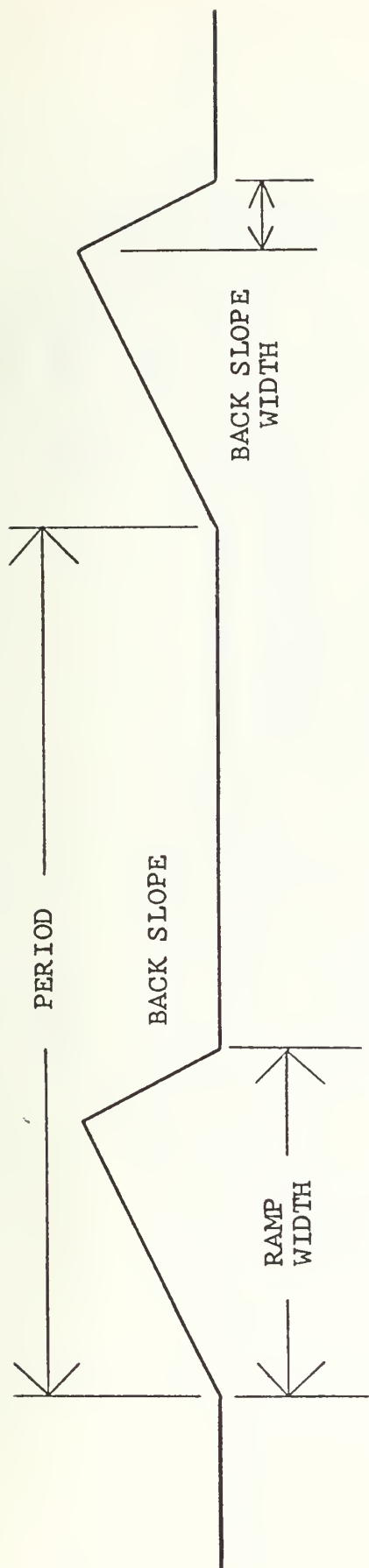


STANDARD RAMP SIGNAL

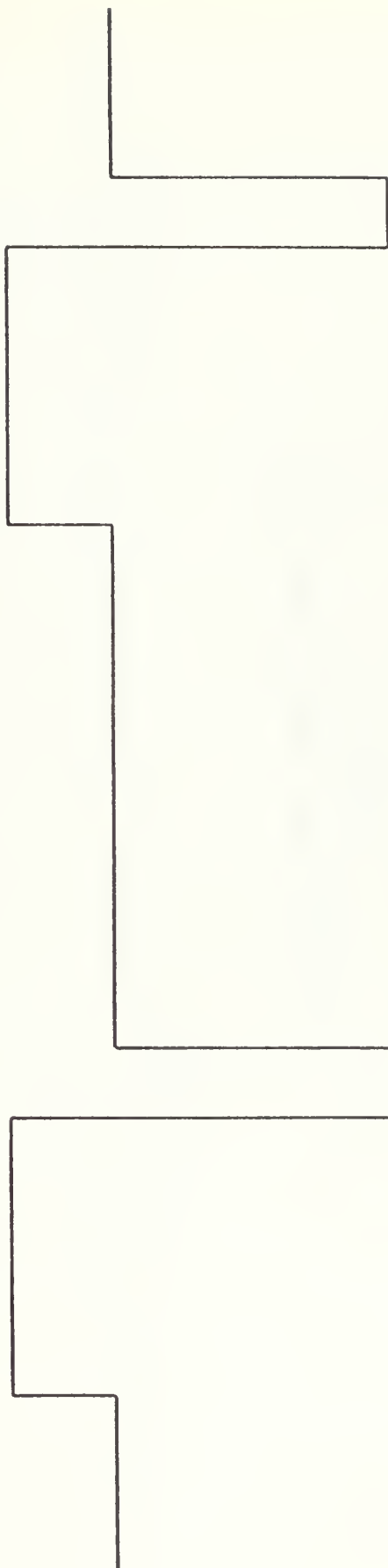


DIFFERENTIATED STANDARD RAMP SIGNAL

FIGURE 4.

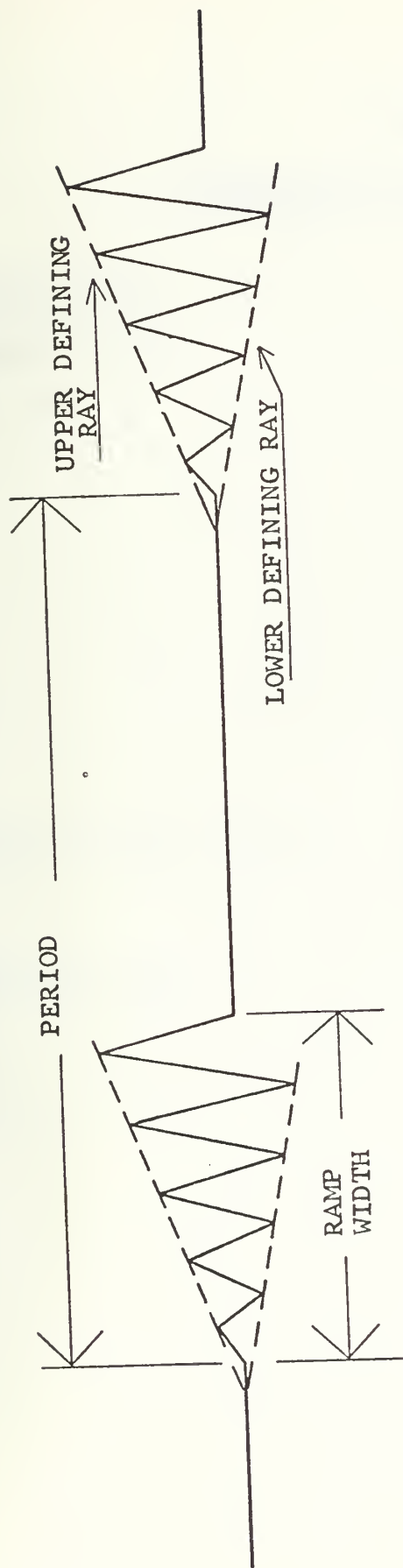


ASYMMETRICAL RAMP SIGNAL

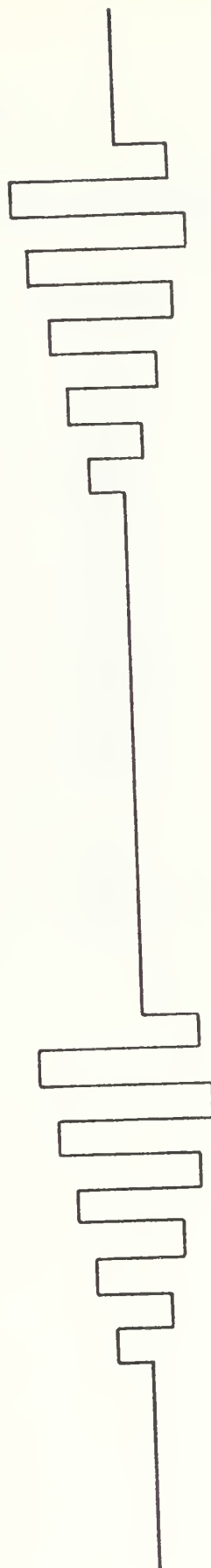


DIFFERENTIATED ASYMMETRICAL RAMP SIGNAL

FIGURE 5.



COMPLEX RAMP SIGNAL



DIFFERENTIATED COMPLEX RAMP SIGNAL

FIGURE 6.

TABLE I.

SKEWNESS AND COEFFICIENT OF EXCESS OF
DIFFERENTIATED TEMPERATURE SIGNALS

<u>INVESTIGATOR</u>	<u>SKEWNESS</u>	<u>C.E.</u>
BOSTON (1971)	-0.013	20.3
	0.195	17.1
	0.140	21.4
	0.002	22.6
	-0.082	13.6
	0.596	22.8
	0.203	12.2
	0.307	13.4
	0.315	32.0
	0.171	13.9
	0.673	30.7
	0.039	15.5
	0.286	18.1
	0.251	11.0
	0.257	12.3
	0.051	6.0
GIBSON <u>et. al.</u> (1970)	0.40	40
	0.72	35
	0.48	34
	0.72	22
GURVICH (1967)		15 - 1400!

IV. RESULTS

The standard ramp signal proved to be a poor representation of the temperature signal. For an appropriate c.e. the skewness was positive but much too large; about five. This agrees with the results obtained by Gibson et.al.(1971) from a similar model. The asymmetrical ramp was no improvement. With this signal a large positive c.e. was accompanied by a large negative skewness. This signal proved to be of some value apart from its intended use and is discussed in Section VI.

The complex ramp signal showed more favorable results. Not only can compatible skewness and c.e. be found but the signal can be adjusted so that skewness and c.e. vary almost independently. A more detailed analysis of the individual signals follows. It should be kept in mind that while a direct signal model is the final product, the different model theories were tested by the statistics of the differentiated signal. Therefore, the following results apply to the statistics of the differentiated signal.

TABLE II.

VARIATION OF DIFFERENTIATED RAMP SIGNAL
WITH PERIOD (FIGURE 7)

PERIOD	RAMP SLOPE	RAMP WIDTH	S.	C.E.
10			0.408	-1.83
20			1.45	0.250
30			2.15	2.65
40	2.0	4.0	2.63	4.90
80			3.98	13.8
100			4.70	20.0
200			6.48	40.0
400			8.49	70.0

Note here that skewness and c.e. both increase with increasing period but they never simultaneously achieve the correct values required by the models.

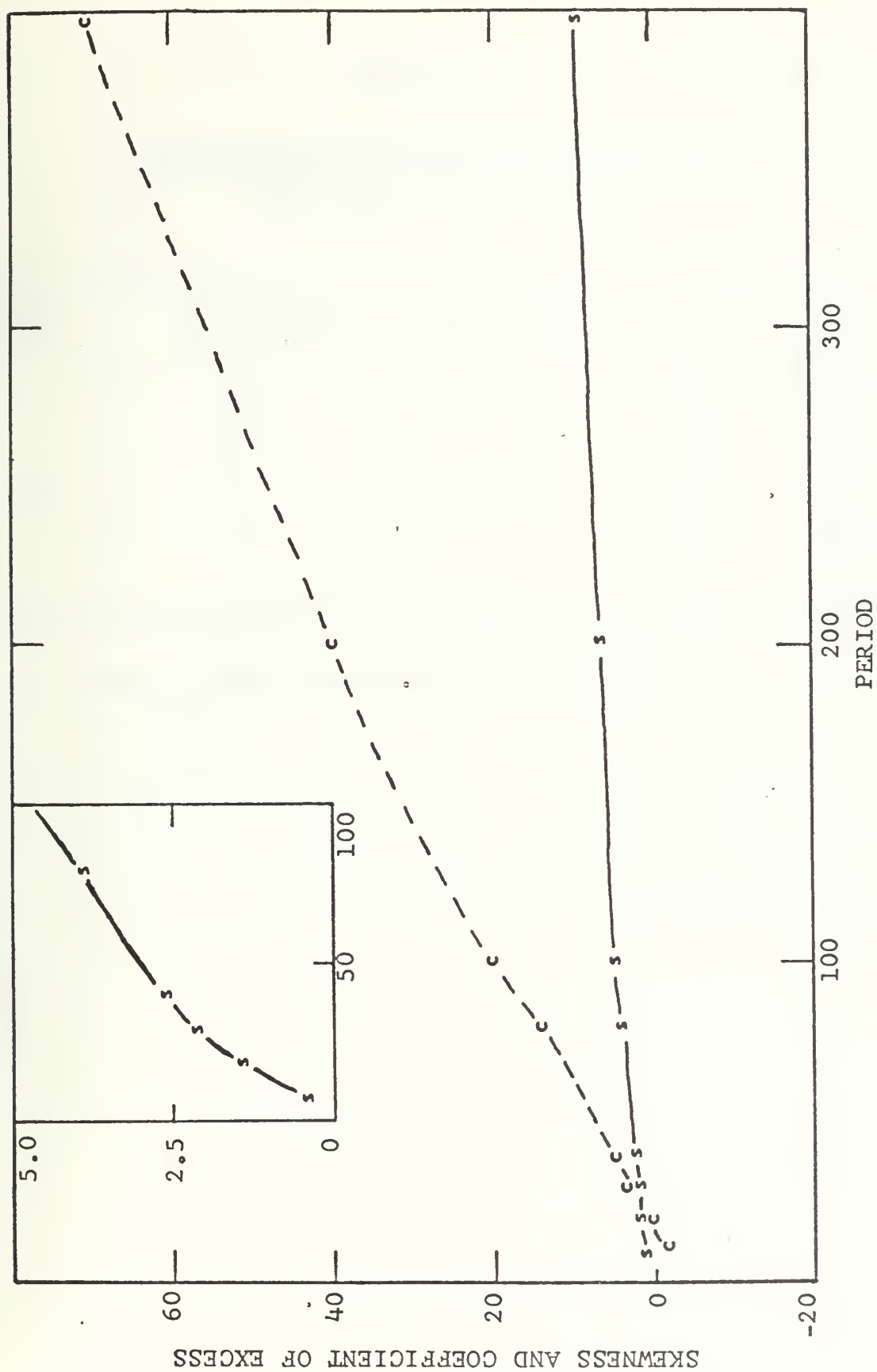


FIGURE 7. Variation of Standard Ramp Signal with Period
(Ramp Slope = 2.0, Ramp Width = 4.0)

TABLE III.

VARIATION OF DIFFERENTIATED RAMP SIGNAL
WITH RAMP SLOPE (FIGURE 9)

PERIOD	RAMP SLOPE	RAMP WIDTH	S.	C.E.
40	0.1	4.0	2.67	5.12
	0.5		2.67	5.12
	1.0		2.67	5.12
	5.0		2.67	5.12

S. and c.e. are independent of ramp slope.

TABLE IV.

VARIATION OF DIFFERENTIATED RAMP SIGNAL
WITH RAMP WIDTH (FIGURE 8)

PERIOD	RAMP SLOPE	RAMP WIDTH	S.	C.E.
40	2.0	2.0	4.13	15.1
		3.0	3.23	8.41
		4.0	2.67	5.11
		5.0	2.27	3.14
		6.0	1.96	1.85
		7.0	1.71	0.929

Here the results are similar to those obtained with a varying period. Although values of s and $c.e.$ can be achieved with the standard ramp signal that are respectively commensurate with measured values from actual signals, the values of s and $c.e.$ are not simultaneously compatible with measured signals and hence this signal is discarded as an appropriate model.

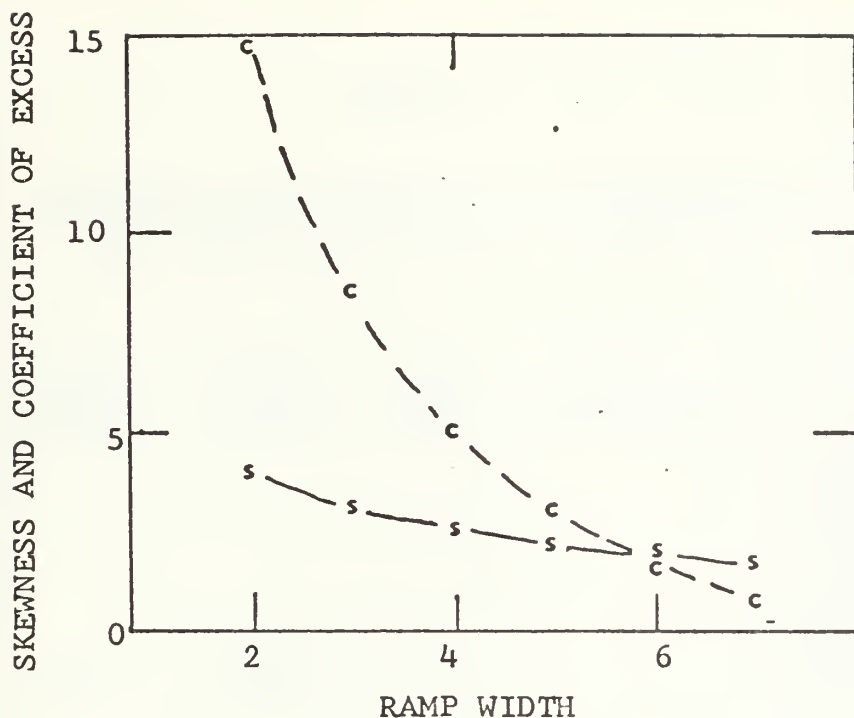


FIGURE 8. Variation of Standard Ramp Signal with Ramp Width (Period = 40, Ramp Slope = 2.0)

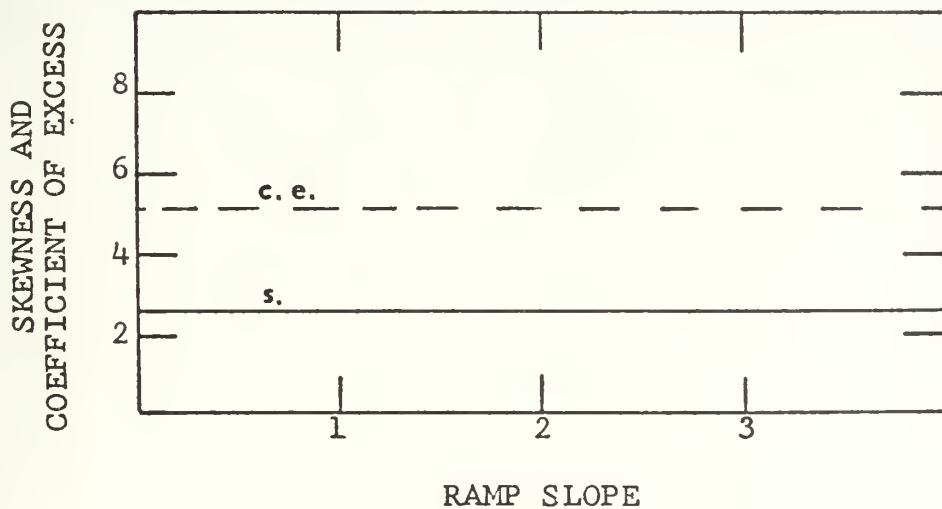


FIGURE 9. Variation of Standard Ramp Signal with Ramp Slope (Period = 40, Ramp Width = 4.0)

TABLE V.

VARIATION OF DIFFERENTIATED ASYMMETRICAL
RAMP SIGNAL WITH PERIOD (FIGURE 10)

PERIOD	BACK SLOPE	FRONT SLOPE	RAMP WIDTH	BACK SLOPE WIDTH	S.	C.E.
10					-3.77	13.2
30					-4.64	21.6
50					-6.00	38.0
100	-1.5	0.167	10	1	-8.48	78.9
300					-14.7	243
500					-18.9	403

Although c.e. values are achieved that agree with actual signal values, the skewness values are not only too large in absolute value but negative instead of the small positive values desired.

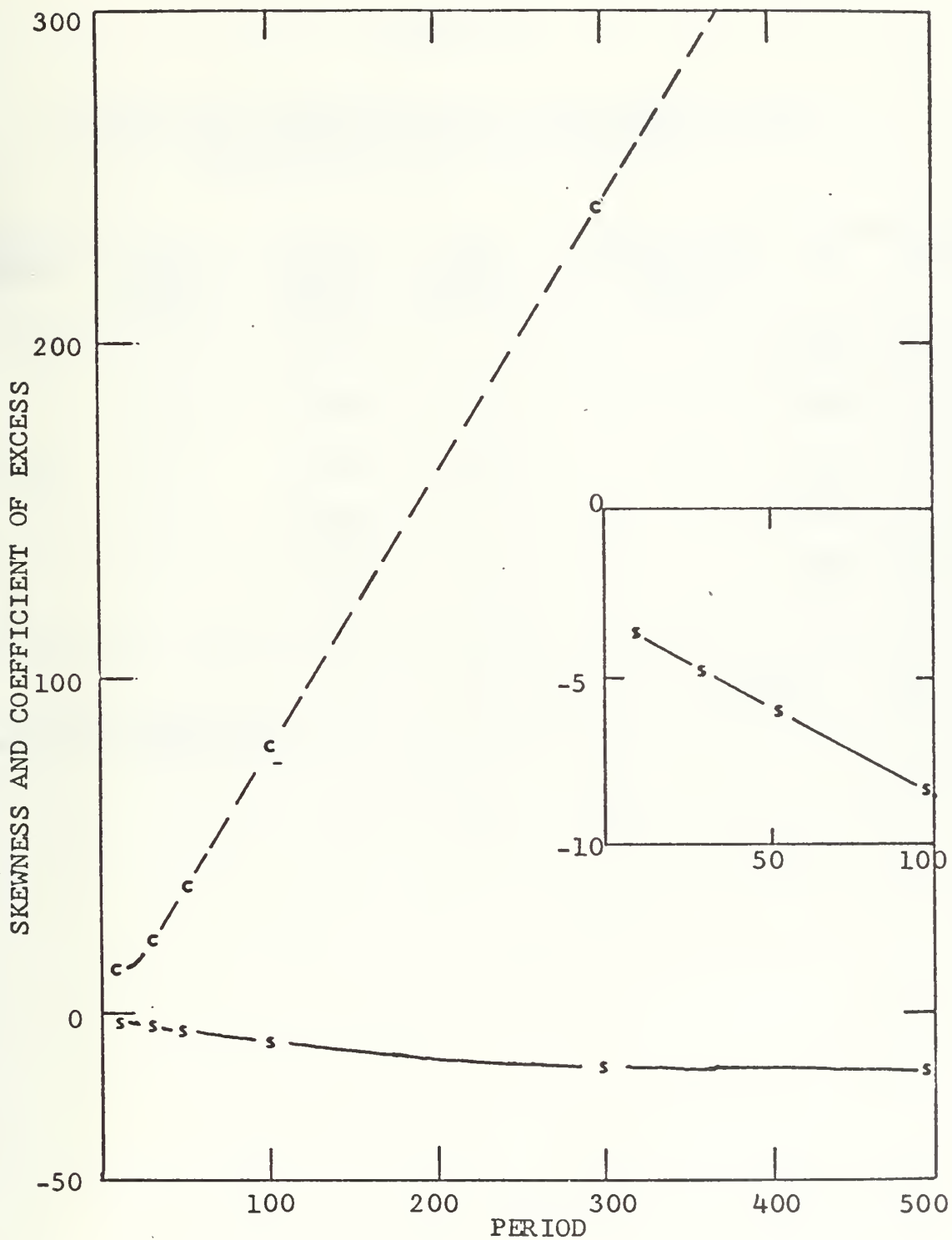


FIGURE 10. Variation of Asymmetrical Ramp Signal with Period
 (Back Slope = -1.5, Ramp Width = 10, Back Slope Width = 1)

TABLE VI.

VARIATION OF DIFFERENTIATED ASYMMETRICAL RAMP
SIGNAL WITH BACK SLOPE (FIGURE 12)

PERIOD	BACK SLOPE	FRONT SLOPE	RAMP WIDTH	BACK SLOPE WIDTH	S.	C.E.
100	-0.10	0.011	10	1	-8.43	78.1
	-0.50	0.056			-8.43	78.1
	-1.0	0.10			-8.43	78.1
	-1.5	0.144			-8.43	78.1
	-1.9	0.189			-8.43	78.1

Once again the slope of the signal has no effect on the modeling statistics.

TABLE VII.

VARIATION OF DIFFERENTIATED ASYMMETRICAL RAMP SIGNAL
WITH RAMP WIDTH (FIGURE 11)

PERIOD	BACK SLOPE	FRONT SLOPE	RAMP WIDTH	BACK SLOPE WIDTH	S.	C.E.
100	-1.5	0.30	6		-7.30	67.0
		0.25	7		-7.72	70.8
		0.21	8		-8.02	73.8
		0.19	9	1	-8.25	76.2
		0.17	10		-8.43	78.1
		0.08	20		-9.23	87.3
		0.05	30		-9.49	90.4

These statistics are not compatible with measured values.
The skewness is too large in absolute value and negative in
sign.

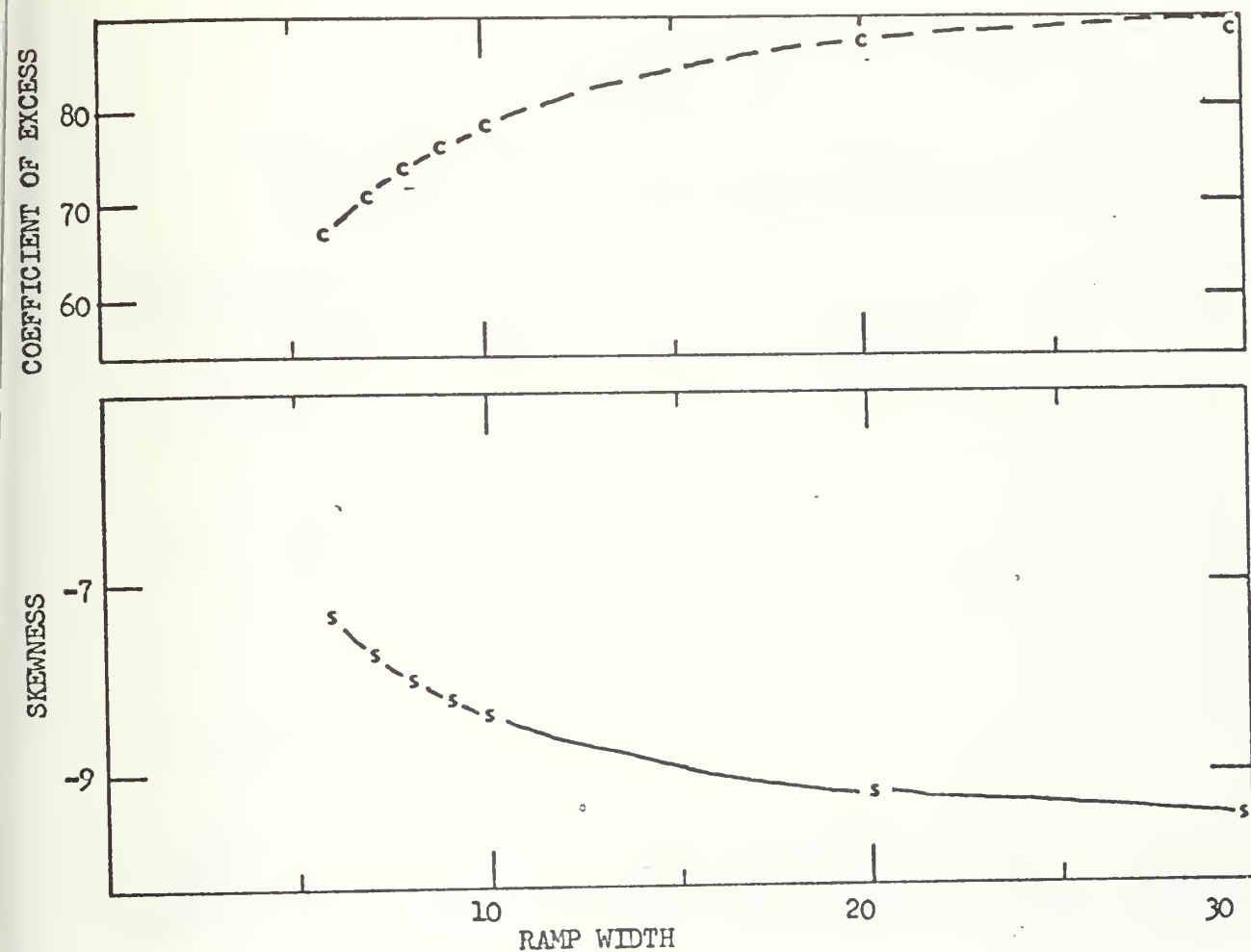


FIGURE 11: VARIATION OF ASYMMETRICAL RAMP SIGNAL WITH RAMP WIDTH
(PERIOD = 100, BACK SLOPE = -1.5, BACK SLOPE WIDTH = 1)

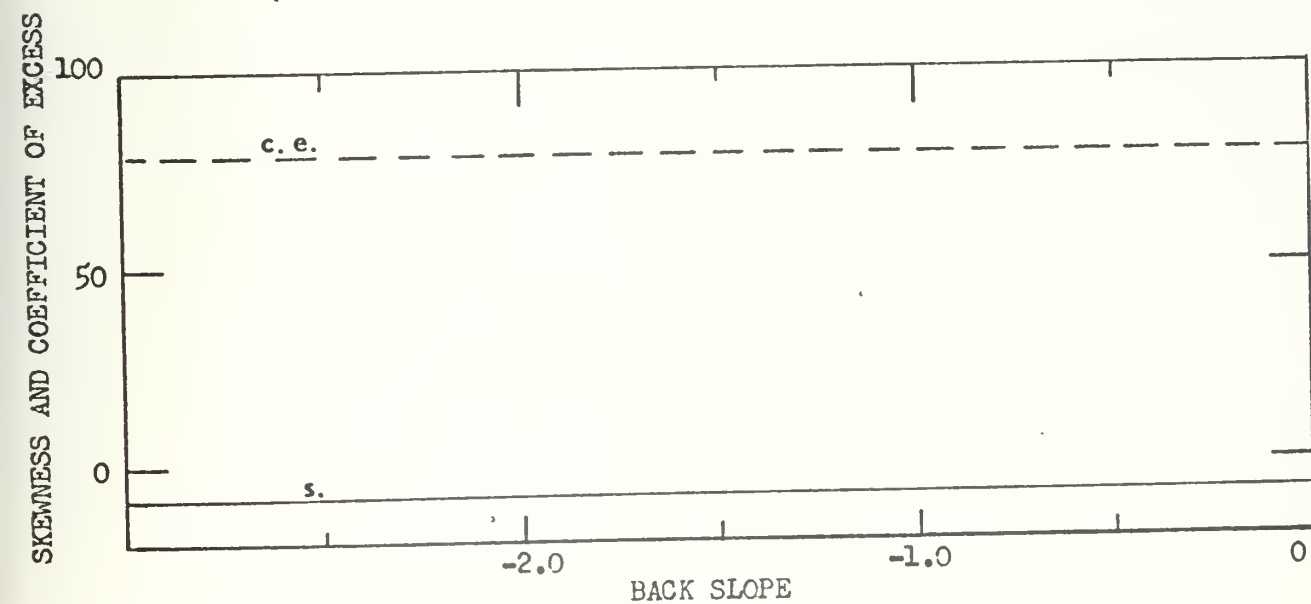


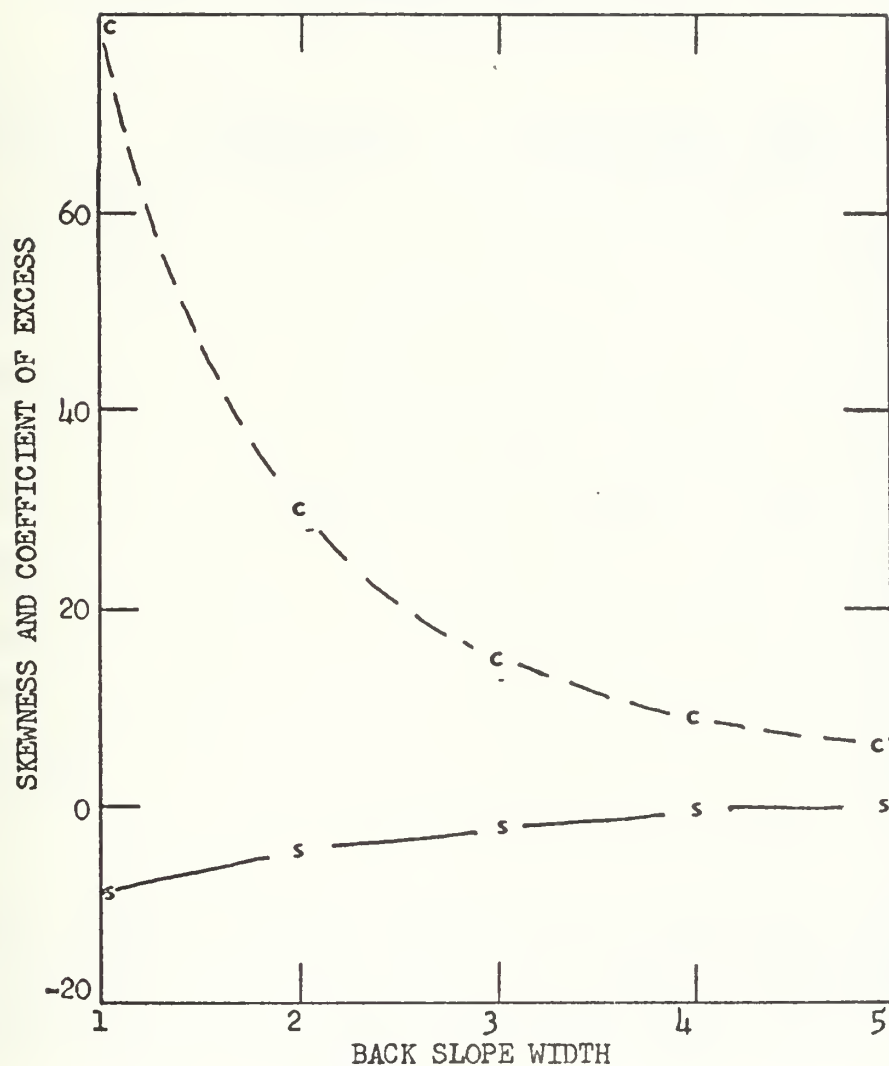
FIGURE 12: VARIATION OF ASYMMETRICAL RAMP SIGNAL WITH BACK SLOPE
(PERIOD = 100, RAMP WIDTH = 10, BACK SLOPE WIDTH = 1)

TABLE VIII.

VARIATION OF DIFFERENTIATED ASYMMETRICAL RAMP
SIGNAL WITH BACK SLOPE WIDTH (FIGURE 13)

PERIOD	BACK SLOPE	FRONT SLOPE	RAMP WIDTH	BACK SLOPE WIDTH	S.	C.E.
100	-1.5	0.167	10	1	-8.48	78.9
		0.375		2	-4.77	29.8
		0.643		3	-2.77	14.8
		1.0		4	-1.30	8.78
		1.5		5	0.0	7.0

Note that the skewness finally becomes non-negative (zero) but the c.e. is too low and the shape of the signal is that of a teepee, not a ramp. Therefore, due to the negative skewness inherent in this signal, it is discarded as a possible model.



VARIATION OF ASYMMETRICAL RAMP SIGNAL WITH BACK SLOPE WIDTH
(PERIOD = 100, BACK SLOPE = -1.5, RAMP WIDTH = 10)

FIGURE 13.

TABLE IX.

VARIATION OF DIFFERENTIATED COMPLEX RAMP SIGNAL
WITH PERIOD (FIGURE 14)

PERIOD	UPPER BASIC SLOPE	LOWER BASIC SLOPE	RAMP WIDTH	S.	C.E.
40				0.046	-1.27
80				0.064	0.459
100				0.072	1.32
200				0.102	5.64
300	0.8	-0.4	40	0.124	9.71
400				0.145	14.3
600				0.175	22.4
800				0.201	30.2
1000				0.229	40.2

This signal closely approximates actual measured values for periods in the range of 800 to 1000. This appears to be an excellent model for typical atmospheric temperature signals during unstable conditions. Now the effect of the remaining parameters will be examined.

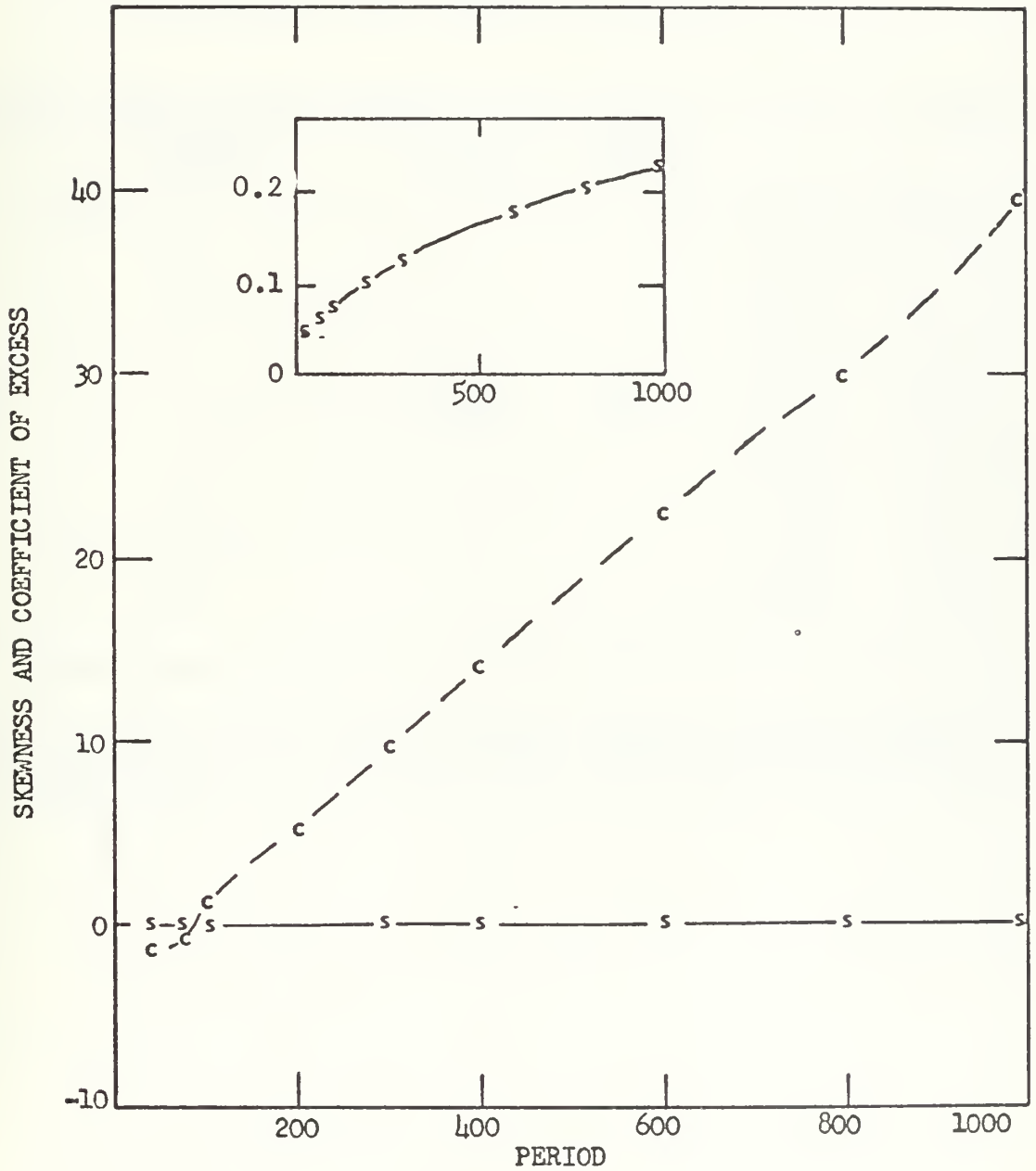


FIGURE 14: VARIATION OF COMPLEX RAMP SIGNAL WITH PERIOD
 (UPPER BASIC SLOPE = 0.8, LOWER BASIC SLOPE = -0.4, RAMP WIDTH = 10)

TABLE X.

VARIATION OF DIFFERENTIATED COMPLEX RAMP SIGNAL
WITH UPPER BASIC SLOPE (FIGURE 15)

PERIOD	UPPER BASIC SLOPE	LOWER BASIC SLOPE	RAMP WIDTH	S.	C.E.
800	0.4			0.208	30.6
	0.8			0.201	30.2
	1.2			0.175	30.2
	1.6	-0.4	40	0.153	30.2
	2.0			0.134	30.2
	2.4			0.119	30.2
	50			0.008	30.7

The coefficient of excess remains almost constant while the skewness ranges over values not unlike those encountered in real signals.

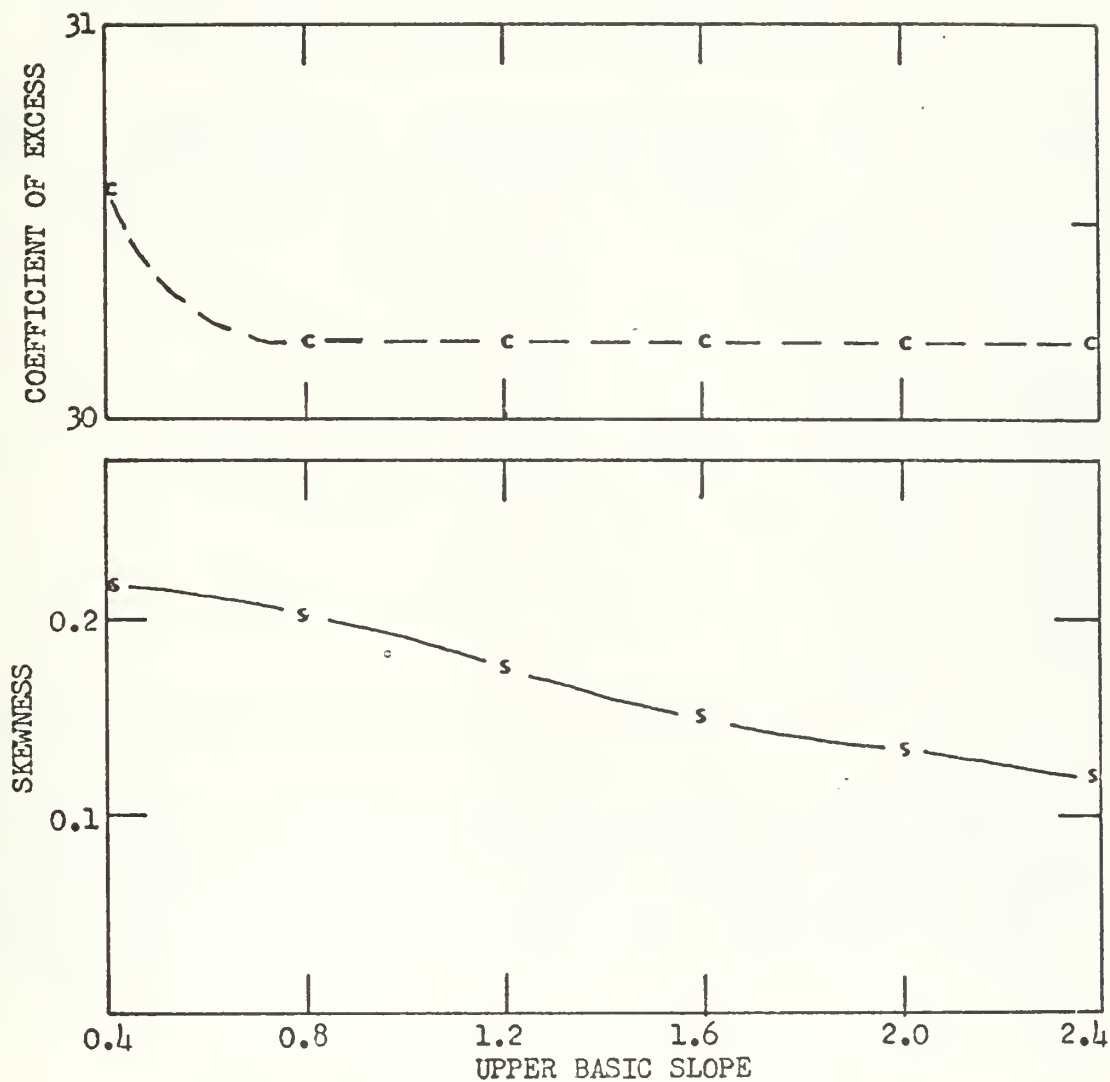


FIGURE 15: VARIATION OF COMPLEX RAMP SIGNAL WITH UPPER BASIC SLOPE
(PERIOD = 800, LOWER BASIC SLOPE = -0.4, RAMP WIDTH = 40)

TABLE XI.

VARIATION OF DIFFERENTIATED COMPLEX RAMP SIGNAL
WITH LOWER BASIC SLOPE (FIGURE 16)

PERIOD	UPPER BASIC SLOPE	LOWER BASIC SLOPE	RAMP WIDTH	S.	C.E.
800	0.8	0.6	40	-10.3	227
		0.4		- 2.29	58.2
		0.2		- 0.488	34.6
		0.0		0.0	30.7
		-0.2		0.153	30.2
		-0.4		0.201	30.2
		-0.6		0.211	30.4

The values of s and c.e. obtained when the lower basic slope is positive fluctuate greatly but when the lower basic slope becomes negative the c.e. becomes almost constant, about 30, and the skewness stabilizes near 0.2. Therefore, it is concluded that the model of a temperature signal has a lower basic slope less than zero.

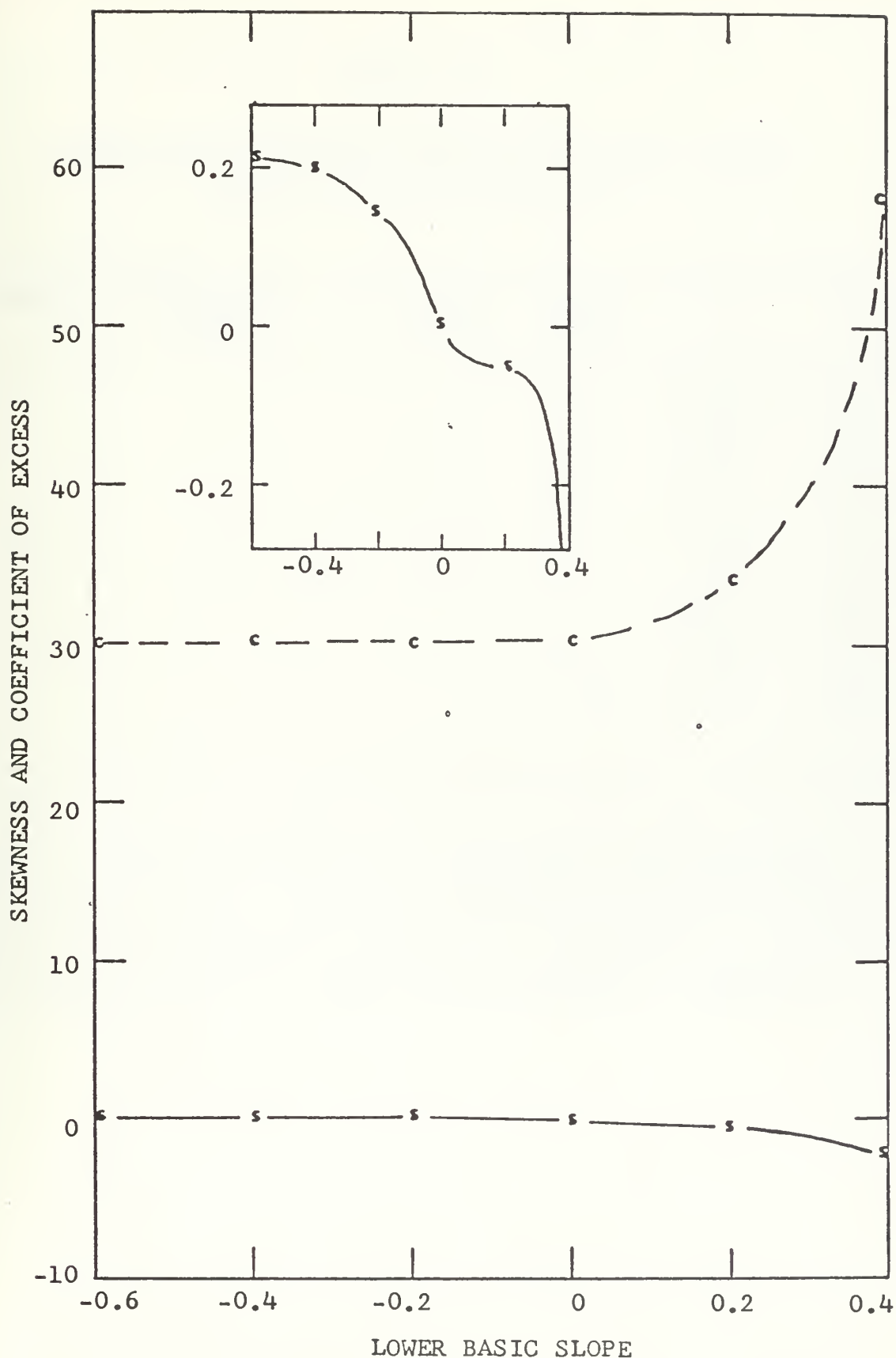


FIGURE 16: VARIATION OF COMPLEX RAMP SIGNAL WITH LOWER BASIC SLOPE (PERIOD = 800, UPPER BASIC SLOPE = 0.8, RAMP WIDTH = 40)

TABLE XII.

VARIATION OF DIFFERENTIATED COMPLEX RAMP SIGNAL
WITH RAMP WIDTH (FIGURE 17)

PERIOD	UPPER BASIC SLOPE	LOWER BASIC SLOPE	RAMP WIDTH	S.	C.E.
800	0.8	-0.4	40	0.201	30.2
			50	0.145	23.8
			60	0.111	19.5
			70	0.089	16.3
			80	0.073	14.0
			90	0.061	12.1
			100	0.052	10.6

The effect of varying the ramp width has much the same effect as varying the period. Decreasing the ramp width causes s and $c.e.$ to increase; likewise an increase in period has similar results. These two adjustments however do not produce equal changes in s and $c.e.$ For example, in TABLE IX there is a signal with skewness of 0.145 and a $c.e.$ of 14.3, while from TABLE XII a signal with skewness of 0.145 has a $c.e.$ of 23.8.

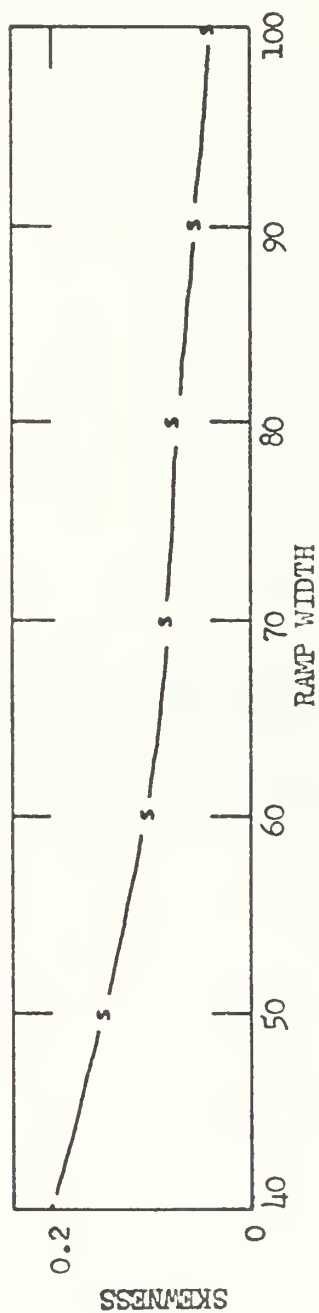
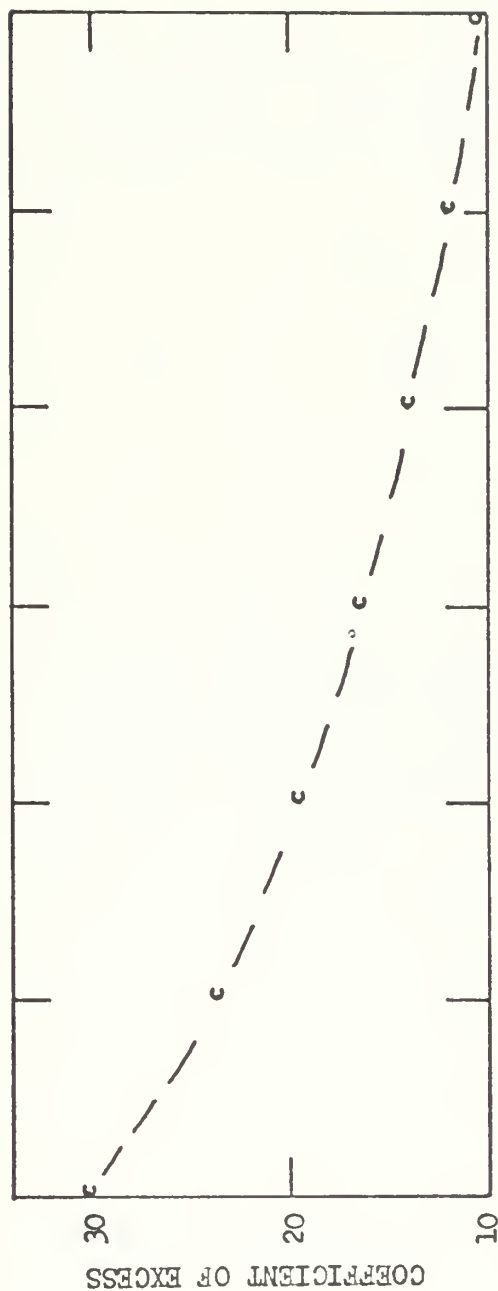


FIGURE 17: VARIATION OF COMPLEX RAMP SIGNAL WITH RAMP WIDTH
(PERIOD = 800, UPPER BASIC SLOPE = 0.8, LOWER BASIC SLOPE = -0.4)

TABLE XIII.

VARIATION OF DIFFERENTIATED COMPLEX RAMP SIGNAL
WITH PERIOD AND RAMP WIDTH

PERIOD	UPPER BASIC SLOPE	LOWER BASIC SLOPE	RAMP WIDTH	S.	C.E.
200			10	0.702	28.1
400			20	0.389	30.3
800	0.8	-0.4	40	0.201	30.2
1600			80	0.099	28.5
3200			160	0.047	24.8

TABLE XIII is listed for the information of the reader and as an aid to those who might want to model temperature signals. In each successive entry in TABLE XIII the period and ramp width have been doubled. As previously noted, this has the effect of doubling the frequency of the internal teepees. Also, it is a means of changing the skewness while keeping the c.e. relatively constant.

The preceding tables have not been an attempt to list all the variations possible with the different models, but to examine how various parameters affect the models and to determine which model, if any, is the best representation of atmospheric temperature signals. As previously noted, the complex ramp signal was selected as the best representation. Obviously there exists an infinite number of possible variations and given the actual values of a signal together with the previous tables one should be able to model most of the atmospheric temperature signals encountered in an unstable atmosphere.

The complex ramp provides a coarse and a fine "tuning" mechanism for the model. The ramp width and/or the period can be adjusted to the desired c.e. value with an s value near that desired and then the skewness tuned by adjusting the upper basic slope while the coefficient of excess remains constant. Additionally, the model of the differentiated complex ramp (Figure 6) is remarkably similar to the actual differentiated signal (Figure 1).

V. CONCLUSIONS

The results of this study indicate successful accomplishment of the objective; which was to model a temperature signal from its statistical parameters, skewness, and coefficient of excess. Furthermore, additional insight was gained into the actual structure of temperature signals.

Although the study was not exhaustive it does indicate that one cannot attribute the observed values of skewness and coefficient of excess in the differentiated temperature signal entirely to the external dimensions and frequency of the ramps. Instead one must look at the internal structure of the ramp itself. The ramp is composed of a great many fluctuating high frequency saw-teeth which gradually increase in amplitude giving an overall impression of a relatively gradual rising ramp. The fluctuations are presumably due to mixing or entrainment by the diffuse leading edge of the manifesting plume. The saw-teeth actually extend below the ambient temperature level. This is not readily apparent when examining temperature strip charts but can be attributed to the mechanical response of the recorder and/or sensing system. The internal saw-teeth cause the variation in skewness while the width or frequency of the entire ramp causes variation in c.e. Therefore, given the skewness and coefficient of excess of a temperature signal, a model can be constructed with the exact statistics of the original signal.

VI. RECOMMENDATIONS FOR FURTHER STUDY

A natural extension of this thesis would be an attempt to model actual signals. This would probably require not only an examination of strip chart recordings but also an investigation of the signal's digital representation.

While the asymmetrical ramp signal proved unsatisfactory as a temperature model, in an extreme variation it's statistics were remarkably similar to those of a velocity signal. When the back slope width was only slightly smaller than half the entire ramp width a small negative skewness and a c.e. of near 20 was noted. Several of these results are listed in TABLE XIII. Except for a shape that more resembles a teepee than a ramp, this signal should behave exactly like the previously noted asymmetrical ramp signal. An inspection of a velocity signal indicates that this teepee-like representation is not a bad resemblance. However, it should also be noted that the same results can be achieved with a complex ramp signal whose lower basic slope is greater than zero but necessarily less than the upper basic slope (TABLE XI). Perhaps a more accurate model would be a combination of the two, where high frequency fluctuations are inscribed between two asymmetrical ramps similar to those noted above such that the ramps have the same widths but different heights, i.e., front slopes and back slopes.

If this model proved successful it would hopefully inherit the characteristic of the complex ramp whereby the skewness and c.e. could be adjusted independently.

TABLE XIV.

VARIATION OF A DIFFERENTIATED VELOCITY
SIGNAL WITH RAMP WIDTH

PERIOD	BACK SLOPE	FRONT SLOPE	RAMP WIDTH	BACK SLOPE WIDTH	S.	C.E.
100	-1.5	1.5	4		0.0	22.0
		1.0	5		-1.53	20.3
		0.75	6	2.0	-2.89	22.0
		0.60	7		-3.59	24.1

THIS PROGRAM COMPUTES THE SKEWNESS (SKEW) AND COEFFICIENT OF EXCESS (CE) FOR A COMPLEX RAMP SIGNAL WITH A PERIOD OF 800, AN UPPER BASIC SLOPE OF 0.8, A LOWER BASIC SLOPE OF -0.4 AND A RAMP WIDTH OF 40. PARAMETERS BOXED WITH *'S ARE THE VARIABLES OF THE SIGNAL. A DO LOOP INSERTED BEFORE STATEMENT 5 AND LOOPEED THROUGH STATEMENT 90 WILL ALLOW ONE OR MORE OF THE VARIABLES TO BE INCREMENTED.

INITIALIZE DATA

```

      REAL*4 LSLOPE
      DIMENSION X(10000)
5     DO 10 I=1,10000
10    X(I)=0.0
      NO=10000
      M=1
      CODE=10**10
      *******
      * INT=800
      * USLOPE=0.8
      * LSLOPE=-0.4
      * WIDTH=40
      *******
      IND=0
      N1=2
      N2=WIDTH/2

```

COMPUTE COMPLEX SIGNAL

```

      DO 50 K=1,10000

```

COMPUTE POSITIVE SLOPES

```

      X(1+IND)=2.*USLOPE
      DO 25 J=N1,N2
25    X(2*J-1+IND)=2.*J*USLOPE-(2.*J-1)*LSLOPE

```

COMPUTE NEGATIVE SLOPES

```

      N3=N2-1
      X(2+IND)=3.*LSLOPE-2.*USLOPE
      DO 35 J=N1,N3
35    X(2*J+IND)=(2.*J+1)*LSLOPE-2.*J*USLOPE
      X(2*N2+IND)=-2.*N2*USLOPE
      IND=IND+INT

```

CHECK IF SIGNAL ARRAY IS FILLED

```

      IF(2*N2+IND.GT.10000) GO TO 75
50    CONTINUE

75    CALL MISR(NO,M,X,CODE,XBAR,STD,SKEW,CE,R,N,A,B,S,IER)
80    WRITE (6,200) INT,USLOPE,LSLOPE,WIDTH,SKEW,CE
85    CONTINUE
90    WRITE (6,300) X
200   FORMAT ('0', 'INT=', I5, 2X, 'USLOPE=', F7.3, 2X, 'LSLOPE=',
1     F7.3, 2X, 'WIDTH=', F5.1, 2X, 'SKEW=', F8.3, 2X, 'CE=', F8.3, /)
300   FORMAT (1X, 'DATA SIGNAL FOLLOWS', /, 100(10F10.3/))
      STOP
      END

```


10 MISR
20 MISR
30 MISR
40 MISR
50 MISR
60 MISR
70 MISR
80 MISR
90 MISR
100 MISR
110 MISR
120 MISR
130 MISR
140 MISR
150 MISR
160 MISR
170 MISR
180 MISR
190 MISR
200 MISR
210 MISR
220 MISR
230 MISR
240 MISR
250 MISR
260 MISR
270 MISR
280 MISR
290 MISR
300 MISR
310 MISR
320 MISR
330 MISR
340 MISR
350 MISR
360 MISR
370 MISR
380 MISR
390 MISR
400 MISR
410 MISR
420 MISR
430 MISR
440 MISR
450 MISR
460 MISR
470 MISR
480 MISR

.....
SUBROUTINE MISR
PURPOSE
COMPUTE MEANS, STANDARD DEVIATIONS, SKEWNESS AND KURTOSIS,
CORRELATION COEFFICIENTS, REGRESSION COEFFICIENTS, AND
STANDARD ERRORS OF REGRESSION COEFFICIENTS WHEN MISSING DATA
ARE SKIPPED IN COMPUTING THE STATISTICS. IN THE CASE OF IF
CODE, THE PAIR OF VALUES ARE SKIPPED IF
EITHER ONE OF THEM ARE MISSING.
USAGE
CALL MISR (NO,M,X,CODE,XBAR,STD,SKEW,CURT,R,N,A,B,S,IER)
DESCRIPTION OF PARAMETERS
NO - NUMBER OF OBSERVATIONS
M - NUMBER OF VARIABLES
X - INPUT DATA MATRIX OF SIZE NO X M. WHICH CONTAINS A NUMERIC
CODE - MISSING DATA CODE. THE CODE HAVING VALUES EQUAL TO THE CODE
FOR A GIVEN VARIABLE WILL BE DROPPED FOR COMPUTATIONS. MEANS
XBAR - OUTPUT VECTOR OF LENGTH M CONTAINING STANDARD DEVI-
STD - OUTPUT VECTOR OF LENGTH M CONTAINING SKEWNESS
SKEW - OUTPUT VECTOR OF LENGTH M CONTAINING KURTOSIS
CURT - OUTPUT MATRIX OF PRODUCT-MOMENT CORRELATION
R - COEFFICIENTS. SINCE THE MODE OF PAIRS OF OBSERVATIONS USED
MATRIX ONLY. (STOPAGE MODE 1)
N - IS SYMMETRIC. (STORAGE OF COEFFICIENTS
A - OUTPUT MATRIX OF NUMBER OF COEFFICIENTS. ONLY THE
IN COMPUTING THE CORRELATION OF THE
(STOPAGE MODE 1)
B - OUTPUT MATRIX (M BY M) CONTAINING INTERCEPTS OF
REGRESSION LINES (A) OF THE FORM $Y=A+BX$. THE FIRST
SUBSCRIPT OF THE MATRIX REFERS TO THE INDEPENDENT
VARIABLE AND THE SECOND TO THE INTERCEPT OF THE
REGRESSION LINE. A(1,3) CONTAINS THE INTERCEPT OF VARIABLE 1
IS INDEPENDENT LINE AND STORED IN A VECTOR FORM. NOTE
THAT MATRIX A IS STORED IN A VECTOR FORM.
B - OUTPUT MATRIX (M BY M) CONTAINING REGRESSION

CC


```

COEFFICIENTS (B) CORRESPONDING TO THE VALUES OF
INTERCEPTS CONTAINED IN THE OUTPUT MATRIX A.
- OUTPUT MATRIX (M BY M) CONTAINING STANDARD ERRORS
OF REGRESSION COEFFICIENTS CORRESPONDING TO THE
COEFFICIENTS CONTAINED IN THE OUTPUT MATRIX B.
IER - 0, NO ERROR.
1, IF NUMBER OF NON-MISSING DATA ELEMENTS FOR J-TH
VARIABLE IS TWO OR LESS. IN THIS CASE, STD(J),
SKW(J), AND CURT(J) ARE SET TO 10**75. ALL
VALUES OF R, A, B, AND S RELATED TO THIS VARIABLE
ARE ALSO SET TO 10**75.
2, IF VARIANCE OF J-TH VARIABLE IS LESS THAN
10**(-20). IN THIS CASE, STD(J), SKW(J), AND
CURT(J) ARE SET TO 10**75. ALL VALUES OF R, A,
B, AND S RELATED TO THIS VARIABLE ARE ALSO SET TO
10**75.

REMARKS
THIS SUBROUTINE CANNOT DISTINGUISH A BLANK AND A ZERO.
THEREFORE, IF A BLANK IS SPECIFIED AS A MISSING DATA CODE IN
INPUT CARDS, IT WILL BE TREATED AS 0 (ZERO).

SUBROUTINES AND FUNCTION SUBPROGRAMS REQUIRED
NONE

METHOD
LEAST SQUARES REGRESSION LINES AND PRODUCT-MOMENT CORRE-
LATION COEFFICIENTS ARE COMPUTED.
.....

```

```

SUBROUTINE MISR (ND,M,X,CODE,XBAR,STD,SKW,CURT,R,N,A,B,S,IER)
DIMENSION X(1),CODE(1),XBAR(1),STD(1),SKW(1),CURT(1),R(1),N(1)
DIMENSION A(1),B(1),S(1)

      COMPUTE MEANS
IER=0
L=0
DO 20 J=1,M
  FN=0.0
  XBAR(J)=0.0
  DO 15 I=1,N0
    L=L+1
    IF(X(L)-CODE(J)) 12, 15, 12

```



```

12 FN=FN+1.0
13 XBAR(J)=XBAR(J)+X(L)
15 CONTINUE
16 IF(FN) 16, 16, 17
17 XBAR(J)=0.0
18 GO TO 20
19 XBAR(J)=XBAR(J)/FN
20 CONTINUE

```

C C C

SET-UP WORK AREAS AND TEST WHETHER DATA IS MISSING

```

L=0
DO 55 J=1,M
  LIJ=NO*(J-1)
  SUMW(J)=0.0
  CURT(J)=0.0
  KI=MA*(J-1)
  KJ=J-M
  DO 54 I=1,J
    KI=KI+1
    KJ=KJ+M
    SUMW(J)=0.0
    SUMY=0.0
    TI=0.0
    TJ=0.0
    TII=0.0
    TIJ=0.0
    TIJ=0.0
    NIJ=0
    LI=NO*(I-1)
    LIJ=LIJ+1
    L=L+1
    LI=LI+1
    LIJ=LIJ+1
    IF(X(LI)-CODE(I)) 30, 38, 30
    IF(X(LJ)-CODE(J)) 35, 38, 35

```

30 BOTH DATA ARE PRESENT

C C C

```

35 XX=X(LI)-XBAR(I)
  YY=X(LJ)-XBAR(J)
  TI=TI+XX
  TII=TII+XX*XX
  TIJ=TIJ+YY
  TIJ=TIJ+YY*YY
  NIJ=NIJ+1

```

MISR 950
MISR 960
MISR 970
MISR 980
MISR 990
MISRI1000
MISRI1010
MISRI1020
MISRI1030
MISRI1040
MISRI1050
MISRI1060
MISRI1070
MISRI1080
MISRI1090
MISRI1100
MISRI1110
MISRI1120
MISRI1130
MISRI1140
MISRI1150
MISRI1160
MISRI1170
MISRI1180
MISRI1190
MISRI1200
MISRI1210
MISRI1220
MISRI1230
MISRI1240
MISRI1250
MISRI1260
MISRI1270
MISRI1280
MISRI1290
MISRI1300
MISRI1310
MISRI1320
MISRI1330
MISRI1340
MISRI1350
MISRI1360
MISRI1370
MISRI1380
MISRI1390
MISRI1400
MISRI1410
MISRI1420

MISRI430
MISRI440
MISRI450
MISRI460
MISRI470
MISRI480
MISRI490
MISRI500
MISRI510
MISRI520
MISRI530
MISRI540
MISRI550
MISRI560
MISRI570
MISRI580
MISRI590
MISRI600
MISRI610
MISRI620
MISRI630
MISRI640
MISRI650
MISRI660
MISRI670
MISRI680
MISRI690
MISRI700
MISRI710
MISRI720
MISRI730
MISRI740
MISRI750
MISRI760
MISRI770
MISRI780
MISRI790
MISRI800
MISRI810
MISRI820
MISRI830
MISRI840
MISRI850
MISRI860
MISRI870
MISRI880
MISRI890
MISRI900

```

SUMX=SUMX+X(LI)
SUMY=SUMY+X(LJ)
IF(I-J) 38, 37, 37
37 SKEW(J)=SKEW(J)+YY**3
38 CURT(J)=CURT(J)+YY**4
CONTINUE

      COMPUTE SUM OF CROSS-PRODUCTS OF DEVIATIONS
C
C
C
      IF(NIJ) 40, 40, 39
      FN=NIJ
      R(L)=TIJ-TI TJ/FN
      N(L)=NIJ
      TII=TI*TI/FN
      TJJ=TJJ-TJ TJ/FN

      COMPUTE STANDARD DEVIATION, SKEWNESS, AND KURTOSIS
C
C
C
      IF(I-J) 47, 41, 47
      IF(NIJ-2) 42, 42, 43
      IER=1
      R(L)=1.0E75
      A(KI)=1.0E75
      B(KI)=1.0E75
      S(KI)=1.0E75
      GO TO 45

      STD(J)=R(L)
      R(L)=1.0
      A(KI)=0.0
      B(KI)=1.0
      S(KI)=0.0

      IF(STD(J)-(1.0E-20)) 44, 44, 46
      IER=2
      STD(J)=1.0E75
      SKEW(J)=1.0E75
      CURT(J)=1.0E75
      GO TO 55

      WORK=STD(J)/FN
      SKEW(J)=(SKEW(J)/FN)/(WORK*SQR(WORK))
      CURT(J)=((CURT(J)/FN)/WORK**2)-3.0
      STD(J)=SQR(STD(J)/(FN-1.0))
      GO TO 55

      COMPUTE REGRESSION COEFFICIENTS
C
C
C

```


MISR1910
 MISR1920
 MISR1930
 MISR1940
 MISR1950
 MISR1960
 MISR1970
 MISR1980
 MISR1990
 MISR2000
 MISR2010
 MISR2020
 MISR2030
 MISR2040
 MISR2050
 MISR2060
 MISR2070
 MISR2080
 MISR2090
 MISR2100
 MISR2110
 MISR2120
 MISR2130
 MISR2140
 MISR2150
 MISR2160
 MISR2170
 MISR2180
 MISR2190
 MISR2200
 MISR2210
 MISR2220
 MISR2230
 MISR2240
 MISR2250
 MISR2260
 MISR2270
 MISR2280
 MISR2290
 MISR2300

```

47 IF(NIJ-2) 48,48,50
48 I=1
49 R(L)=1.0E75
    A(KI)=1.0E75
    B(KI)=1.0E75
    S(KI)=1.0E75
    A(KJ)=1.0E75
    B(KJ)=1.0E75
    S(KJ)=1.0E75
    GO TO 54
C
50 IF(TII-(1.0E-20)) 52,52,51
51 IF(TJJ-(1.0E-20)) 52,52,53
52 I=2
    GO TO 49
C
53 SUMX=SUMX/FN
    SUMY=SUMY/FN
    B(KI)=R(L)/TII
    A(KI)=SUMY-B(KI)*SUMX
    R(KJ)=R(L)/TJJ
    A(KJ)=SUMX-B(KJ)*SUMY
C
C      COMPUTE CORRELATION COEFFICIENTS
R(L)=R(L)/(SQRT(TII)*SQRT(TJJ))
C
C      COMPUTE STANDARD ERRORS OF REGRESSION COEFFICIENTS
RR=R(L)**2
SUMX=(TJJ-TJJ*RR)/(FN-2)
S(KI)=SQRT(SUMX/TII)
SUMY=(TII-TII*RR)/(FN-2)
S(KJ)=SQRT(SUMY/TJJ)
C
54 CONTINUE
55 CONTINUE
C
    RETURN
    END
  
```


BIBLIOGRAPHY

1. Boston, N. E. J., Some Features of Temperature Fluctuations in the Atmospheric Boundary Layer, paper presented at American Physical Society Division of Fluid Dynamics Twenty-Fourth Annual Meeting, San Diego, California, 22-24 November 1971.
2. Boston, N. E. J., "Some Statistics of High Wave Number Temperature and Velocity Fluctuations in the Atmospheric Boundary Layer," Bull. of APS, p. 1312 (Abstract only), Nov. 1971.
3. Gibson, C. H., Friehe, C. A., and McConnel, S. D., Measurements of Sheared Turbulent Scalar Fields, paper presented at AGARD Specialists' Meeting on "Turbulent Shear Flows," London, England, 13-15 September 1971.
4. Gill, T. E., Analysis of Temperature and Velocity Fluctuations in the Atmospheric Boundary Layer, M. S. Thesis, Naval Postgraduate School, Monterey, California, March 1971.
5. Kaimal, J. C. and Businger, J. A., "Case Studies of a Convective Plume and a Dust Devil," Applied Meteorology, v. 9, p. 612-620, August 1970.
6. Kolmogorov, A. N., "A Refinement of Previous Hypotheses Concerning the Local Structure of Turbulence in a Viscous Incompressible Fluid at High Reynolds Number," J. Fluid Mech., v. 13, p. 77-81, May 1962.
7. Kolmogorov, A. N., "The Local Structure of Turbulence in Incompressible Viscous Fluid for Very Large Reynolds Numbers," Doklady ANSSSR, v. 30, p. 301-305, 1941.
8. Lumley, J. L. and Panofsky, H. A., The Structure of Atmospheric Turbulence, Interscience, 1964.
9. Safley, G. W., Investigation on the Temperature Fluctuations and Incidence of Micro-thermals in the Air Adjacent to Natural Water Waves, M. S. Thesis, Naval Postgraduate School, Monterey, California, March 1972.
10. Sokol, E. S., Use of Correlation Techniques in Automatic Detection of Thermal Plumes in the Air Layer Adjacent to Natural Water Waves, M. S. Thesis, Naval Postgraduate School, Monterey, California, June 1971.

11. Stewart, R. W., "Turbulence and Waves in a Stratified Atmosphere," Radio Science, v. 4, No. 12, p. 1269-1278, Dec. 1969.
12. Stewart, R. W., Wilson, J. R., and Burling, R. W., "Some Statistical Properties of Small Scale Turbulence in an Atmospheric Boundary Layer," J. Fluid Mech., v. 41, Part I, p. 141-159, 1970.
13. Taylor, R. S., "Thermal Structures in the Lower Layers of the Atmosphere," Austral. J. Physics, v. 11, p. 168-176, 1958.

INITIAL DISTRIBUTION LIST

	No. Copies
1. Defense Documentation Center Cameron Station Alexandria, Virginia 22314	2
2. Library, Code 0212 Naval Postgraduate School Monterey, California 93940	2
3. Department of Oceanography Naval Postgraduate School Monterey, California 93940	3
4. Oceanographer of the Navy The Madison Building 732 N. Washington Street Alexandria, Virginia 22314	1
5. Dr. Ned Ostenso Code 480D Office of Naval Research Arlington, Virginia 22217	1
6. Asst. Professor N. E. J. Boston, Code 58Bb Department of Oceanography Naval Postgraduate School Monterey, California 93940	5
7. Asst. Professor K. L. Davidson, Code 51Ds Department of Meteorology Naval Postgraduate School Monterey, California 93940	1
8. Asst. Professor A. L. Schoenstadt, Code 53Zh Department of Mathematics Naval Postgraduate School Monterey, California 93940	1
9. LT Edward M. Kline, USN Class 39 Naval Destroyer School Newport, Rhode Island 02840	1

DOCUMENT CONTROL DATA - R & D

(Security classification of title, body of abstract and indexing annotation must be entered when the overall report is classified)

1. ORIGINATING ACTIVITY (Corporate author)		2a. REPORT SECURITY CLASSIFICATION	
Naval Postgraduate School Monterey, California 93940		Unclassified	
		2b. GROUP	
3. REPORT TITLE			
A Statistical Model of Atmospheric Temperature Signals			
4. DESCRIPTIVE NOTES (Type of report and inclusive dates)			
Master's Thesis; March 1972			
5. AUTHOR(S) (First name, middle initial, last name)			
Edward M. Kline			
6. REPORT DATE		7a. TOTAL NO. OF PAGES	7b. NO. OF REFS
March 1972		63	13
8a. CONTRACT OR GRANT NO.		9a. ORIGINATOR'S REPORT NUMBER(S)	
b. PROJECT NO.			
c.		9b. OTHER REPORT NO(S) (Any other numbers that may be assigned this report)	
d.			
10. DISTRIBUTION STATEMENT			
Approved for public release; distribution unlimited.			
11. SUPPLEMENTARY NOTES		12. SPONSORING MILITARY ACTIVITY	
		Naval Postgraduate School Monterey, California 93940	
13. ABSTRACT			
<p>The "ramp" is an often observed feature in temperature fluctuations during unstable atmospheric conditions. It is characterized by a gradual increase in temperature followed by a sudden drop to an ambient level. This ramp clearly distinguishes temperature signals from other turbulence signals such as velocity. Three different ramp-type atmospheric temperature fluctuations and their derivatives are constructed and statistically examined for the parameters skewness and coefficient of excess. These statistical values are compared with values obtained from actual signals. The "complex ramp signal" was found to represent these quite well. Skewness and coefficient of excess for this signal could be altered almost independently of each other. The complex ramp is constructed by inscribing nearly symmetrical consecutive triangles within two envelope rays of constant but different slopes such that the two envelope rays approximate a ramp function.</p>			

14.

KEY WORDS

LINK A

LINK B

LINK C

ROLE

WT

ROLE

WT

ROLE

WT

Thermal Plume

Skewness

Coefficient of Excess

Atmospheric Temperature Signals

Model Temperature Signals

Micro-thermals

Turbulence



Thesis
K5837

134025

c.1 Kline

A statistical model
of atmospheric temper-
ature signals.

T
K
C

Thesis
K5837

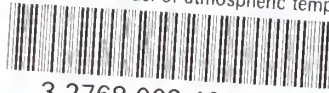
134025

c.1 Kline

A statistical model
of atmospheric temper-
ature signals.

thesK5837

A statistical model of atmospheric tempe



3 2768 002 10629 6

DUDLEY KNOX LIBRARY